NASA TECHNICAL MEMORANDUM

NASA TM X- 73977

NASA TM X-73977

ASSESSMENT OF VARIABLE-CYCLE ENGINES FOR MACH 2.7 SUPERSONIC TRANSPORTS: A STATUS REPORT

by S. J. Morris and W. E. Foss, Jr.
NASA Langley Research Center

and

J. W. Russell
Vought Corporation
Hampton Technical Center

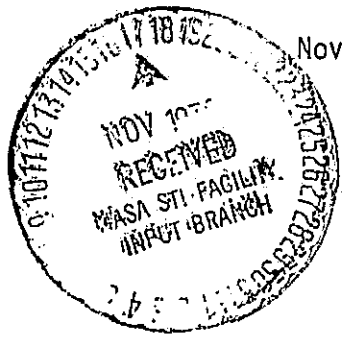

November 1, 1976

National Aeronautics and Space Administration

Langley Research Center
Hampton, Virginia 23665

1. Report No.	2. Government Accession No.	3. Recipient's Catalog No.
NASA TM X-73977		

4. Title and Subtitle	5. Report Date
ASSESSMENT OF VARIABLE-CYCLE ENGINES FOR MACH 2.7 SUPERSONIC TRANSPORTS: A STATUS REPORT	November 1, 1976
	6. Performing Organization Code 31.600

7. Author(s)	8. Performing Organization Report No.
S. J. Morris, W. E. Foss, Jr., NASA Langley Research Center, and J. W. Russell, Vought Corporation	
	10. Work Unit No.
9. Performing Organization Name and Address	
NASA Langley Research Center Hampton, Virginia 23665	11. Contract or Grant No.
	13. Type of Report and Period Covered
12. Sponsoring Agency Name and Address	Technical Memorandum
National Aeronautics and Space Administration Washington, DC 20546	14. Sponsoring Agency Code

15. Supplementary Notes

16. Abstract

This report evaluates each of three proposed SCAR propulsion systems in terms of aircraft range for a fixed payload and take-off gross weight with a design cruise Mach number of 2.7. The effects of various noise and operational restraints are determined and sensitivities to some of the more important performance variables are presented for the most probable design noise and operational restraint case. Critical areas requiring new or improved technology for each cycle are delineated. This report describes the status of the NASA SCAR M=2.7 design studies as of its publication.

17. Key Words (Suggested by Author(s))	18. Distribution Statement
Variable Cycle Engines, SCAR, Supersonic Transport, System Studies	Unclassified - Unlimited

19. Security Classif. (of this report)	20. Security Classif. (of this page)	21. No. of Pages	22. Price*
UNCLASSIFIED	UNCLASSIFIED	57	$4.25

* For sale by the National Technical Information Service, Springfield, Virginia 22161

ASSESSMENT OF VARIABLE-CYCLE ENGINES FOR MACH 2.7 SUPERSONIC TRANSPORTS; A STATUS REPORT

S. J. Morris and W. E. Foss, Jr.
NASA Langley Research Center

and

J. W. Russell
Vought Corporation
Hampton Technical Center

SUMMARY

The NASA Supersonic Cruise Aircraft Research (SCAR) program has sponsored extensive work to define technology improvements which could lead to an economically and environmentally viable advanced supersonic transport. One element of the program involved the generation of a multitude of advanced conventional and variable-cycle "paper" engines by the engine manufacturers and screening them in a typical transport mission to find the most promising engine cycles. These latter cycles were evaluated by the airplane manufacturers in more detailed mission studies with the results that three promising candidate engine cycles were identified for further study and refinement. The present report evaluates each of these three proposed SCAR propulsion systems in terms of aircraft range for a fixed payload and takeoff gross weight with a design cruise Mach number of 2.7. The effects of various noise and operational restraints are determined and sensitivities to some of the more important design variables are presented for the most probable design case. Critical areas requiring new or improved technology for each cycle are delineated. This report describes the status of the NASA SCAR M = 2.7 design studies as of its publication date.

INTRODUCTION

With the cancellation of the United States Supersonic Transport (SST) program in 1971, an enormous concentrated developmental effort for civil supersonic flight technology came to an abrupt halt in the U.S.A. This did not deter dedicated engineers from examining the problems which led to the demise of the U.S. SST and prophesying new technology requirements for a second-generation SST which would lead to substantial improvement in performance, economics, safety, and social acceptability. A paper presented by Nichols later in 1971 (Ref. 1) indicated that substantial range improvements were possible with advances in aerodynamics, structures, materials, propulsion, and flight control within the restraints imposed by takeoff noise considerations. Although the gains shown were those for an advanced dry turbojet engine equipped with a noise suppressor, Nichols called for inventiveness to define a variable-cycle engine to "have

the airflow characteristics at takeoff of the turbofan combined with the good cycle efficiency of the turbojet in supersonic cruise." As a result of studies such as this, NASA in 1972 elected to establish a low-keyed effort now known as the Supersonic Cruise Aircraft Research program (SCAR) to define, foster, and fund research efforts to develop the technology needed to support any future attempt to build a second-generation SST.

Shortly after the start of the SCAR program, Swan (Ref. 2) indicated that a weight reduction equivalent to that of the entire payload would have been possible for the U.S. SST had a variable-cycle engine been available. The implication was that the variable-cycle engine would be capable of generating a large airflow in a turbofan mode with low specific trust levels to meet both the takeoff field length and regulated noise level without a suppressor. It would cruise supersonically as a dry turbojet and would maintain high inlet flows when operating at part power to eliminate throttle dependent spillage, bypass, and boattail drag. Swan further made the point that "the propulsive system concept must be treated as an entity, including inlet and exhaust systems such that reduced weight, drag, and complexity of these latter components may be traded for increased weight and complexity of the variable cycle." At about the time Swan presented his paper, the results of Boeing's JT8D variable bypass engine test (Ref. 3) were made known to the staff of NASA. This test demonstrated the ability to increase airflow 70 percent and vary the bypass ratio from 1.1 to 3.5 through the use of an air inverter valve. Partly as a result of this information, the on-going SCAR engine studies performed under contract with General Electric and Pratt & Whitney, and directed by NASA Lewis Research Center, were expanded to include studies of a family of unconventional variable-cycle engines. The results of these studies, which are still underway, are described in Reference 4.

The purpose of this paper is to assess, on an integrated mission basis, the performance of three variable-cycle engine concepts resulting from the on-going SCAR program and to delineate those areas of technology which must be developed to achieve such performance. The engine cycles selected have differing degrees of variablility and complexity as well as differing advantages and disadvantages with respect to each other. The figure of merit employed is the maximum range achieved at a cruise Mach number of 2.62 on a hot day for a given takeoff gross weight and payload. The baseline comparisons are made for vehicles with optimum performance-sized engines and for vehicles with engines sized to meet FAR noise regulations both with and without suppression. Comparisons are made with the GE4, the engine selected for the U.S. SST, to illustrate the improvements afforded by advanced engine technology. Comparisons are also made showing the range sensitivity of these supersonic cruise vehicles to changes in operating weight empty, propulsion system weight, supersonic cruise specific fuel consumption (SFC), SFC for the entire mission, supersonic cruise lift drag ratio (L/D) and L/D for the entire mission. The sensitivities are made using the performance necessary to meet FAR 36 with suppression case as a baseline.

The engine data are as supplied by the engine manufacturers, and no independent evaluation of the validity of the data or ability to perform as specified has been made. Where opinions are expressed in the paper, they represent those of the authors alone.

Part of the information presented in this report was previously described at the 48th meeting of the AGARD Propulsion and Energetics Panel (Ref. 5) in September 1976.

ENGINE SELECTION AND DESCRIPTION

Many engine cycles of both conventional and unconventional types were generated and examined by the Pratt & Whitney and General Electric companies under the auspices of the NASA/SCAR program. Each of these engines was screened in a mission simulation program to pinpoint the more desirable cycles. Mission simulation was a necessary tool since it is well known that comparisons of the usual performance parameters of thrust-weight ratio, specific fuel consumption, installed thrust level are not necessarily indicative of the best cycle in view of the conflicting rquirements imposed by noise restraints, weight, thrust margin, and subsonic versus supersonic cruise fuel consumption rates. The performance data of the higher ranked engine cycles were provided to the airplane companies to evaluate in their SCAR-sponsored system studies. Based upon the results of these studies the most promising cycles were further refined and analyzed in more detail by the engine manufacturers. The net result of this iterative process was the definition of three candidate variable-cycle engines of differing degrees of variability. For each of these engines, a technology base available for a certificated engine in the late 1980's was assumed. For conventional engine components, an extrapolation based upon historical data was used by the engine manufacturers to predict weight and performance. For nonconventional components, estimates of performance and weight were based upon results using small-scale models wherever possible and in all cases with a degree of restrained optimism in keeping with an objective of the SCAR to delineate potentially attractive areas for new technology research.

To establish a bench mark against which to assess the performance of these candidate variable-cycle engines the aircraft performance was also generated for the engine selected for the former U.S. SST (the GE4/J5P). It is included to indicate the gains possible due to technology advances since 1969 in conventional components and due to cycle variability. The four engine cycles are briefly described below. Each of the variable-cycle engines have been optimized in terms of overall pressure ratio and fan pressure ratio for a standard day flight Mach number of 2.7 for direct comparison with the GE4 which was designed specifically for this flight Mach number. The engine cycle parameters and performance are listed in Table 1.

Pratt & Whitney - Variable Stream Control Engine

The variable stream control engine (VSCE), shown in Figure 1, is a two-spool duct-burning turbofan employing a convergent-divergent ejector nozzle. In essence, it is similar to the JTF17, the Pratt & Whitney entry for the U.S. SST program but employs a higher turbine inlet temperature, a variable area throat for the primary stream, and a greater degree of variable geometry in

the fan and compressor. The use of this variability permits a more complex throttle schedule to be used. This throttle schedule essentially matches the engine and inlet flow schedule at maximum dry and augmented power settings at all flight Mach numbers to minimize spillage, bypass, and boattail drag. In addition, for takeoff, the primary burner is throttled back with the duct burner lit and full airflow maintained to achieve a tailored exhaust gas velocity profile. This technique maximizes the coannular noise relief at the required takeoff thrust level. A detailed description of the engine and explanation of the coannular noise relief are contained in Reference 6. The VSCE represents a conservative approach toward achieving the objective of a variable-cycle engine. Its performance at both supersonic and subsonic cruise conditions is quite similar to that of a conventional duct-burning turbofan.

Pratt & Whitney - Rear Valve Variable-Cycle Engine

The rear valve variable-cycle engine (RVE) has been found to yield the most attractive application of the air inverter valve concept. It is used as a means of cycle conversion from turbofan to turbojet and vice versa. A description of the air inverter valve and its use in this and other arrangements is given in Reference 3. The operation of the RVE is described in detail in Reference 6 and is briefly reviewed here. The RVE (Fig. 1) is a two-spool nonafterburning engine employing a variable geometry fan and a split low-pressure turbine and incorporates a convergent-divergent ejector nozzle. The air inverter valve functions as a diverter/mixer and is located before the last element of the low-pressure turbine. In the twin turbojet mode, the duct burner is lit and the valve is in the inverting position such that the core flow is bypassed around, and the heated duct flow through the rear low-pressure turbine. In the turbofan mode, the valve is used to mix the unheated duct flow with the core flow before expanding through the rear turbine element. The inner stream nozzle throat is fixed. In the turbojet mode of operation, variation of the outer stream nozzle throat area and fan burner temperature are used to maintain constant corrected airflow at supersonic cruise part power thrust levels. Airflow regulation in the turbofan mode is uniquely defined by turbine inlet temperature since all the flow exits through the fixed area inner stream nozzle throat. Thus, in the turbofan mode a greater degree of spillage must exist compared to the turbojet mode. This is a result of lower fan speed due to the lower flow energy level at the rear turbine because of the mixing of both streams. The RVE exhibits the greatest variability of any variable-cycle engine in this group in that it operates like a turbofan engine at subsonic cruise and as a turbojet at supersonic cruise speeds.

General Electric - Double Bypass Variable-Cycle Engine

The double bypass variable-cycle engine (DBE) is a low bypass-ratio two-spool mixed-flow afterburning turbofan engine. The fan is divided into two separate elements. These elements are designed so that engine air can be

bypassed downstream of each element. The configuration is shown schematically in Figure 1 and is described in detail in Reference 4. The DBE engine used in the present investigation is a later version of the engine described in Reference 4. In this later version, both bypassed streams are mixed and a portion of the mixed flow is exhausted through an auxiliary nozzle in the takeoff and low-speed cruise modes. For takeoff, variable turbomachinery geometry is used to overspeed the fan and increase the airflow approximately 20 percent. This overspeeding in combination with the translating shroud convergent-divergent plug nozzle (Ref. 7) and annular noise relief (Refs. 8 and 9), significantly reduces the jet noise as compared to a conventional C-D nozzle equipped low bypass ratio turbofan engine. The engine throttle modulates the variable stators and bypass flow paths to provide inlet engine airflow match at all flight Mach numbers at both maximum dry and augmented thrust levels and to provide full airflow down to approximately 50 percent of dry thrust. The DBE represents a degree of variability midway between the VSCE and RVE.

General Electric - GE4

The GE4 engine, which is used to illustrate the technology base available in 1969, is a single spool afterburning turbojet equipped with a convergent-divergent two-stage ejector nozzle. The engine has a variable area nozzle and employs a two-position compressor stator schedule. The engine weight and performance parameters were taken from the model specifications for the GE4/J5P for a standard day.

MODELS AND METHODS

A comparison of the various variable-cycle engines can best be achieved if the airplane-engine characteristics are optimized for each of the individual engines. The maximum performance is then obtained subject to the operational restraints imposed by such factors as takeoff field length, noise, approach and takeoff velocity. The techniques used in the present paper to obtain this objective are discussed below. In all cases, the maximum range achieved for a given takeoff gross weight was calculated for a simple 8^{o} C hot day; that is, the temperature at any standard day altitude is increased by 8^{o} C and the speed of sound is calculated for the increased temperature. All other state variables are assumed to be the same as for a standard day. To avoid stagnation temperatures in excess of that of standard day flight Mach number of 2.7, the maximum flight Mach number for the hot day assumption is limited to a value of 2.62.

The figure of merit used to compare the performance of the various engine cycles is the maximum range achieved for a fixed takeoff gross weight and payload.

Airplane

The airplane configuration chosen to "fly" with the candidate engines is shown in Figure 2. It is designed for a cruise Mach number of 2.7 standard day. For maximum aerodynamic efficiency, it incorporates an arrow-wing planform mounting four engines in separate pods aft beneath the wing for favorable interference effects. It has been sized to have a design 8^{o} C hot day range of 7348 km (3968 n. mi.) carrying 292 passengers and equipped with an advanced single-spool nonafterburning turbojet engine. It meets the design range with a takeoff gross weight of 325679 kg (718000 lbm) which is the value assumed throughout this paper.

The airplane characteristics for a wing loading of 352 kg/m^2 (72 lbm/ft^2) are fully described in Reference 10. As a result of recent wind-tunnel tests, more efficient flaps were developed. The use of these flaps enabled the wing loading to be increased to 415 kg/m^2 (85 lb_m/ft^2) and still meet takeoff field length criteria and resulted in improved range. Therefore, the wing area was reduced while maintaining the same aspect ratio. The aerodynamic characteristics were recalculated and the airplane rebalanced. The resulting baseline airplane maximum lift-drag ratio as a function of Mach number is shown in Figure 3. The airplane drag includes that due to both nacelle interference and nacelle skin friction. All other propulsion system drag items are included in the installed engine performance.

A more complete description of the vehicle aerodynamics used in this report may be found in Appendix A. The baseline operating weight empty less that of the propulsion system is 33.8 percent of takeoff gross weight.

Mission Profile

The mission profile flown for each engine is illustrated in Figure 4. Fuel reserve allowance from FAR 121.648 SST Fuel Requirement (tentative standard proposed by FAA) was modified for a change in holding altitude from 457 m (1500 ft) to 4572 m (15000 ft). The effect of changing these reserves to the TWA suggested standard (hold at 3048 m (10000 ft) (ref. 11) or a modified TWA (hold at 4572 m (15000 ft) is also demonstrated for the baseline with suppression case for each engine. The cruise portion of the mission was assumed to be entirely supersonic for the baseline mission. However, the necessity of avoiding sonic boom over populated areas may require a portion of the flight to be conducted at subsonic cruise speeds. This requirement makes the development of a variable-cycle engine especially attractive for supersonic transports. Therefore, two alternate mission profiles were examined which incorporated a 1111-km (600-n. mi.) subsonic cruise range at either the departure or arrival portion of the flight. The subsonic cruise leg is assumed to be at a Mach number of 0.9 at best cruise altitude. The Mach number altitude climb schedule for all-supersonic cruise mission is shown in Figure 5. This schedule has been used in previous studies and has been

checked to insure that it did not cross any flutter boundaries. Full climb thrust was employed during the accelerating climb without any attempt to optimize power management for any given engine cycle.

Engine-Airframe Matching

The relationship between engine size and wing area for maximum range can best be determined through the use of the so-called "thumbprint" or "knothole" diagram. Such a diagram is illustrated in Figure 6 for the RVE engine. Contours of constant range are shown as a function of installed thrust loading and wing loading. The contours were developed with the aid of the computer program described in Reference 12 which generates performance for a matrix of input wing loading and thrust loading values. Engine weight and dimensions are scaled in accordance with information provided with the engine performance decks. The airplane operating weight empty is adjusted for wing loading changes by assuming a constant fuselage and empennage weight and adjusting wing weight as a function of wing loading and engine weight in accord with previously determined parametric scaling laws. The airplane aerodynamic polar diagrams are adjusted for the effects of wing area changes and for the effects of both altitude and nacelle size on skin-friction drag.

Superimposed on the thumbprint diagram are limit lines which represent physical or operational restraints. Areas on the shaded side of each line represent portions of the diagram that violate the constraint. The balanced takeoff field length, excess thrust, approach and takeoff speed limits lines are assigned based on operational consideration at the values shown.

For the case illustrated in Figure 6, the maximum relative range for an all-supersonic cruise mission without noise restraint is limited at the intersection of the takeoff field length and transonic and supersonic excess thrust limit lines. Only a small sector of the knothole diagram bounded by the approach speed, takeoff field length, and supersonic excess cruise thrust meet all operational restraints for airplanes equipped with the RVE. For all engines, the maximum unrestrained range at the eye of the "knothole" is indicated.

ENVIRONMENTAL AND ECONOMIC FACTORS

The ranki g of engine cycles in the SCAR program included projections of engine cost, maintainability, complexity, as well as performance in order to determine the most economically attractive cycle. The economic factors are ignored in this paper because they represent an area of greatest uncertainty. An engine cycle with a clear performance superiority should be economically competitive.

Emissions

The impact of engine emissions upon the design of combustors or duct burners cannot be assessed until such time as emission regulations are set forth; however, the goal of achieving low emissions both in flight and in the vicinity of the airport is of paramount importance. The development of low emission combustors is a problem shared to the same degree by all candidate engines. Projections based upon recent research indicate the possibility that low emission combustors can be developed within the volume and length of current practice. Therefore, the effect on performance of designing low emission combustors for the candidate variable-cycle engine is ignored in this paper.

The development of a low emission duct burner or afterburner presents a more difficult problem particularly with regard to hydrocarbon levels. Burner efficiencies very much higher than those achieved to date are required without sacrificing low-pressure loss performance. In addition, the current on-going research in low emission combustors for today's commercial engines is not directly applicable to burners because the velocity, pressure, and temperature levels are not comparable. However, it is assumed that the optimism expressed by the engine manufacturers is justified and that timely research and development will yield a low emission duct burner or afterburner with no engine performance or weight penalty.

Noise

The environmental factor that has the greatest impact upon engine size is the sideline and/or flyover noise level. To illustrate the effect of noise restraints, the maximum range for each engine has been determined first by means of the "thumbprint" diagram for maximum performance as previously described without consideration of noise. Secondly, the maximum range with noise restraints applied was determined from the "thumbprint" diagram for an engine sized to meet the maximum allowable noise level of 108 EPNdB at either the sideline or flyover measuring point. In this exercise, the variable-cycle engines were sized to meet the noise restraint both with and without suppression due to annular/coannular noise relief. For these variable-cycle engines, no consideration was given to any additional relief made possible through the use of acoustically treated liners or mechanical stream-immersed suppressors in an effort to demonstrate the potential benefits due solely to the annular/coannular effect. The suppression level assumed was provided by the engine manufacturers and was based upon small-scale static acoustic tests. The noise relief varied with throttle setting reaching a value at maximum throttle of 10 EPNdB for the VSCE, 5 EPNdB for the RVE, and 9 EPNdB for the DBE. The GE4, which is used to represent first-generation SST technology, was presumed to be equipped with an 8 EPNdB mechanical suppressor that weighed 7 percent of bare engine weight and created 5 percent net thrust loss at takeoff. This approach was taken presuming the annular noise relief effect was

unrecognized at the time of the planned entry into service. A more complete description of the technique used to predict the noise levels can be found in Appendix B.

PROPULSION SYSTEM PERFORMANCE

Engine performance data supplied by General Electric and Pratt & Whitney for their engine designs provided the net internal thrust and specific fuel consumption (uninstalled performance) at key altitudes, Mach numbers, and power settings. These data reflect only the effects of inlet pressure recovery, nozzle gross thrust coefficient, horsepower extraction, and engine bleed. As noted previously, all propulsion system related drag with the exception of nacelle friction and interference drag are charged to the engine. The drag due to inlet spillage, boundary-layer bleed, bypass, and boattail as functions of power settings were treated as thrust decrements in generating installed engine performance data decks for each engine. The isolated boattail drag as a function of power setting was provided by the engine manufacturers. Additional information on the propulsion system drag for each of the variable cycle engines is shown in Appendix C.

Each of the variable-cycle engines was presumed to operate in conjunction with the inlet described in References 13, 14, and 15. This inlet is of mixed compression axisymmetric type designed for a Mach number of 2.65 and incorporates a translating center body and bleed ports on both cowl and center body to minimize shock-boundary-layer interaction. It is operated in an unstarted (external compression) mode up to a Mach number of 1.6 at which point the shock is swallowed. This inlet is sized to pass 2 percent greater airflow than that required by the engine and bleed system at supersonic cruise on a standard day. The total pressure recovery, bleed flow requirements, and maximum flow schedule as functions of Mach number are presented in Figure 7.

The GE4 is presumed to operate in conjunction with the Boeing-developed inlet whose performance and drag buildup is essentially as given in Reference 2.

The performance for each of the considered engines at the subsonic and supersonic cruise Mach numbers at altitudes above 11 km (36000 ft) are illustrated in Figure 8. Both installed and uninstalled data are plotted to indicate the effect of installation drags at these conditions. The net thrust has been nondimensionalized with respect to each engine's maximum thrust at the given altitude and Mach number to define a thrust ratio. This technique was used to eliminate engine sizing effects.

The installation penalty at the supersonic cruise Mach number is entirely due to bleed drag except for the DBE which has a boattail drag approximately equal to a third of the bleed drag caused by a rearward facing faired step just upstream of the translating shroud. Boattail drag accounts for approximately 70 percent of the installation penalty for all engines at subsonic cruise Mach

number. At this flight condition, however, the DBE with its translating shroud-plug nozzle and high airflow at part power exhibits about half the installation penalty as compared with the VSCE.

At the supersonic cruise Mach number, the minimum installed specific fuel consumption of all engines shown are quite comparable with a maximum difference of approximately 4 percent. At the subsonic cruise Mach number, the spread of the minimum fuel consumption values increases to approximately 20 percent, with the highest bypass ratio engine, RVE, exhibiting the lowest value and the DBE the highest value. The true ranking of these engines, in terms of fuel economy, depends upon the thrust ratio required to balance drag and engine size required to meet the operational restraints and not only upon the indicated minimum value of SFC.

RESULTS AND DISCUSSION

Comparison of the performance of the various engine cycles in terms of maximum range are presented in Figure 9 and 10 to show directly the effects of cycle, noise, and subsonic cruise requirement on range. The incremental range, fuel usages, and propulsion system performance for each of the maximum range configurations are given in Tables II and III. All engines and airframes were sized to meet the operational limitations imposed by takeoff field length, approach velocity, and excess thrust; however, the limitations imposed by the noise criteria were treated separately. To show the effect of noise, the engines were first sized for maximum performance without consideration of takeoff noise level (no noise restraints). The engines were then resized and matched to the airframe to determine the maximum range with a noise limitation of 108 EPNdB without any noise relief due to mechanical or annular/coannular suppression (108 EPNdB, no suppression). Finally, the effect of the assumed suppression levels were included and the engines resized, where necessary, to determine maximum range (108 EPNdB with suppression). Performance with the GE4 engine is also shown for these various noise restraints in order to establish a reference level to demonstrate the benefits from the variable cycle engine technology.

A summary of ranges for the various noise and operation constraints is shown in Table IV. As can be seen from this table, the maximum ranges for the Mach 2.62 all supersonic cruise mission with all operational and noise restraints removed (the "eye of the thumbprint") are 7532 km (4067 n. mi.) for the VSCE, 7908 km (4270 n. mi.) for the RVE, and 6687 km (3611 n. mi.) for the DBE. All engines sized to meet the 108 EPNdB, with suppression case have a range reduction of about 11 percent relative to their maximum unconstrained range. For this case the variation in range between these variable cycle engines was about 15 percent. The lowest range engine in this group was the DBE and its shorter range is primarily due to the higher propulsion system weight.

A 1111-km (600-n. mi.) subsonic cruise to avoid sonic boom at either the departure or arrival portion of the flight for engines sized to satisfy the noise restrictions with the assumed suppression levels included (Fig. 10) indicate relatively small reductions of 3 to 6 percent in range for the variable-cycle engines; however, trip time increased about 20 percent.

Insight to the factors which have a bearing upon the overall performance noted above may be obtained from Figures 11 to 13 as well as from Table II. The DBE uses the greatest amount of fuel and travels farthest during the climb to supersonic cruise for the case of engines selected with no noise restrictions (Fig. 11). As can be seen in Figure 12, the range of the DBE is limited by the excess thrust available in climb. An increase in the afterburner operating temperature might increase its range because the engine could then be sized to meet the takeoff field length and have more fuel onboard for the more efficient supersonic cruise leg. The RVE, which also exhibits a relatively long climb distance, is limited in engine size by both field length and climb thrust. It cannot climb more rapidly to the supersonic cruise point because the presence of the rear valve sets the limit on auxiliary burner temperature. It is interesting to note that the VSCE which is both slightly lighter and exhibits lower specific fuel consumption at both supersonic and subsonic cruise points has 3 percent less range than the RVE. This is a result of the VSCE accelerating in the less efficient maximum augmented power mode at all speeds. Although no attempt was made to optimize the climb throttle schedule, the range of the VSCE improved 1 percent by restricting duct burning during climb to Mach numbers above 0.8.

Both the RVE and DBE engines, as used in this study, are sized by the requirement to meet the noise limit of 108 EPNdB in the suppressed mode for the given runway length. Increasing the takeoff field length limit for either of these engines would result in an insignificant range improvement because the climb thrust requirement would then become the engine sizing parameter. The climb thrust limit is not an absolute operational requirement; however, any reduction in the assumed minimum thrust-to-drag ratio value of 1.2 will adversely affect acceleration capability to start of cruise and increase trip time. The VSCE, on the other hand, is limited only by takeoff field length and not by noise. The sideline noise which is the dominant factor for this engine is actually less than 108 EPNdB and an increase in takeoff field length would permit the use of a smaller engine and a consequent improvement in range. Relaxation of the takeoff field length limit would, therefore, favor the VSCE. For example, the effect of increasing the runway length to 3810 m (12500 ft) is shown in Figure 12. An examination of the 108 EPNdB, with suppression noise constraint indicate that the 3810 m runway length configuration meets this noise requirement at the thrust loadings and wing loadings indicated in Figure 12. Optimization of the flap setting and throttle setting during the takeoff acceleration could offer additional benefits. For the present, the flap setting was fixed during the takeoff.

Extension of the takeoff length from 3200 m (10500 ft) to 3810 m (12500 ft) increases the VSCE range to 7059 km (3812 n. mi.) or about 5 percent, but increases the RVE and DBE by about 1 percent and 2.5 percent, respectively, because the climb cruise thrust margin restraint becomes active for these engines. If the takeoff field length restriction is increased to 3810 m (12500 ft) and the climb cruise thrust margins are removed the ranges of the VSCE, the RVE and the DBE are 7059 km (3812 n. mi.), 7285 km (3934 n. mi.) and 6435 km (3475 n. mi.), respectively, which represent range improvements of 5, 6, and 7 percent, respectively, when compared with the 3200 m (10500 ft) takeoff field length, 108 EPNdB with suppression case.

The effect of modifying the reserve requirements from the FAR 121.648 modified to 4572 m (15000 ft) hold altitude to a TWA suggested reserve schedule (Ref.11). with a hold at 3038 m (10000 ft) is shown in Figure 14. Also shown in Figure 14 is the effect of changing the TWA hold altitude to 4572 m (15000 ft).

The principle difference in the TWA reserve requirement and the baseline requirement is that the TWA reserves specify 5 percent of trip fuel for the in-route fuel reserve while the baseline was set at 7 percent. Detail of these reserve schedules are included in Reference 11.

Range sensitivities for each of the aircraft cases which meet the 108 EPNdB with suppression noise restraints are shown in Figure 15. In this figure, the mission range and percent change in range is shown as a function of percent change in operating weight empty, SFC, supersonic cruise lift-drag ratio, and the lift-drag ratio for the entire mission. The results are similar for each engine with 1 percent change in operating weight empty producing about 2 percent change in range, 1 percent in propulsion system weight equal about 0.5 percent in range, 1 percent in supersonic cruise SFC equal about 1 percent in range, 1 percent in supersonic cruise L/D equal about 1 percent in range, and 1 percent in entire mission L/D equal about 1.25 percent in range. It should be noted that these sensitivities are for the particular configuration considered and should be generalized with great caution.

The VSCE and the RVE exhibit approximately equal range potential yet represent widely divergent variable-cycle concepts. The VSCE is essentially a turbofan engine with controllable primary and secondary nozzle-throat areas which can be scheduled to provide engine-inlet flow match at maximum nonaugmented power over most of the flight spectrum. The RVE, on the other hand, employs a unique flow path schedule which provides a cycle change from what is essentially a relatively high bypass turbofan to a dual turbojet. Unfortunately, it does not exhibit fully the favorable fuel economy of the conventional turbofan at subsonic cruise nor that of the conventional turbojet at the supersonic cruise Mach number. This is a result of the compromise required in the selection of fan pressure ratio. In the turbojet mode, the overall cycle pressure ratio for the bypassed flow turbojet is equal to the fan pressure ratio and is too low for best fuel economy. In the turbofan mode, the fan pressure ratio is too high and the overpressurization and consequent expansion through the rear turbine reduce the thrust potential of the bypass stream due to the additional

rise in entropy through the fan and turbine. In addition, the RVE cannot generate sufficient thrust for takeoff in the turbofan mode, which is desired for reasons of noise, because its air handling capacity is not increased to compensate for its low specific thrust. Thus, for these reasons, the RVE does not meet the full objectives of a variable-cycle engine set forth by Nichols (Ref. 1).

The DBE is the only one of the three considered variable-cycle engines which maintains full engine airflow at the subsonic cruise power setting. The other two variable-cycle engines must spill or bypass from 12 to 21 percent of full throttle airflow. the fixed airflow of the DBE in combination with the translating shroud nozzle, provides throttle independent bypass, spillage, and boattail drag down to one-half of the maximum nonaugmented thrust level. The elimination of throttle dependent drag is one of the goals for variable-cycle engines advocated by Swan (Ref. 2). However, the specific design of the translating shroud incurs a basic boattail drag which, if it were possible to eliminate by redesign, would yield subsonic as well as supersonic cruise specific fuel consumption rates equal to the VSCE. Although the range of the DBE would increase as a result of eliminating the boattail drag, it would not equal that of the VSCE or RVE because of its higher propulsion system weight fraction.

It should be emphasized that the SCAR engine program was undertaken with the goal of determining the potential gains possible for supersonic cruise aircraft equipped with advanced technology engines and if found attractive to foster research on those components critical to achieving that goal. As a group, the variable-cycle engines were found to be superior to the more conventional cycles (Ref. 5). However, the relative ranking of the three variable-cycles considered in this paper does not necessarily reflect the desirability of choosing the highest ranking cycle for development at this time for several reasons. First the cycle choice may depend upon design Mach number. Second, the relaxation of the restrictive takeoff field length would favor the VSCE which is the only cycle whose sizing is strictly limited in range by takeoff field length and not by noise. Third, the rankings ignore the complexity, maintainability, and cost factors and are dependent solely upon achieving the flexibility, performance, and weight assumed for each engine. A study needs to be done to determine the sensitivity of the aircraft range to variations in the assumed engine component performance parameters. This study should also attempt to ascertain the risk involved to achieve the assumed engine component performance. After this study is accomplished a more detailed part by part engine design should be undertaken to determine the engine weight and dimensions. For conventional components such as fans, compressors, combustors, and turbines, the historical background and on-going research and development programs applicable to all types of engines provide a firm base from which to project performance and weight estimates. However, it is necessary to verify

the performance of new and advanced technology items which affect overall engine performance or weight. Some of the more critical items in this category are reviewed below.

A new technology item that has an important influence on the selection of engine size and thus range is the jet noise relief due to the coannular/annular effect. Although this effect was noted many years ago, its potential benefits were not recognized until recently. Small-scale static tests have established the suppression level over a range of bypass and velocity ratios for the coannular nozzle and radius ratios for the annular nozzle and have been used as a base for estimating the relief for the subject engines. The effects of forward velocity, size, and internal stream mixing upon noise suppression levels are as yet not well known. Therefore, NASA has established a phased experimental program to determine their influence upon noise suppression and to provide a firmer base for future noise prediction studies.

The development of a highly efficient secondary burner is a particularly critical item from the standpoint of meeting the anticipated hydrocarbon emission standard as well as its effect upon fuel consumption. Of all the variable-cycle engines, the performance of the VSCE is most vulnerable to duct burner design changes that may be needed to meet the combustion efficiency levels assumed. The higher pressure and temperatures associated with the secondary burners of the other two engine cycles makes the problem of attaining high efficiency only slightly less difficult. To provide insight and guidance, NASA's Experimental Clean Combustor Program was enlarged to include the study of duct burner concepts leading to high efficiency and low emissions.

The variable-cycle engines employ scheduled stator angle settings in both the fan and compressor elements which in combination with spool speed and exhaust nozzle throat area variation are used to essentially match the inlet airflow schedule at maximum turbine inlet temperature. In addition, the stator angles are scheduled to maintain the engine operating line on the fan and compressor maps near regions of best efficiency. For the DBE, as the cycle changes from double to single bypass operation, the compressor must accept approximately 25 percent greater airflow. This produces a difficult design problem of maintaining good efficiency and sufficient stall margin over a wide pumping range. The assumed performance of the DBE depends to a greater degree upon the resolution of this design problem than do the other cycles. Support for a research program in this area has been funded by NASA.

The use of airflow path control valves for cycle flexibility is uniquely identified with the RVE and DBE cycles. Estimates of valve pressure loss for these cycles were based upon model tests, however, the trade-off of component preformance and weight to achieve maximum overall system performance need more refined design and test data. In addition, the losses associated with mixing streams of differing energy levels, the effect of leakage, and; for the RVE, the effect on turbine efficiency of a periodic circumferential temperature variation need to be determined to validate the engine performance estimates.

The SCAR engine studies have resulted in unusual design and control concepts advocated by the engine manufacturers and verified by airplane companies' systems studies. Although they show significant range improvements as compared to the GE4, further improvements may be possible if the propulsion system concept is treated as an entity. To this end, future studies will involve the cooperative effort of the engine and airplane manufacturers to identify means of modifying the inlet, engine cycle, and nozzle by trading component performance and weight to either maximize range or minimize takeoff gross weight.

Finally, it must be noted that this report is just a status report and that significant improvements in the data are expected. For example, the low speed aerodynamic data used in this report has just been updated with recent continuing wind tunnel tests and significant improvements have been discovered. These improvements should reduce the approach speed and shift the takeoff field length down toward the "eye" of the thumbprint. Improvements are also expected when the flap settings and throttle setting are optimized to minimize noise during takeoff. More exact takeoff field length calculations have indicated that the field length in this report are conservative. The use of these improved field length prediction techniques may result in an increased range for the studied configurations. Also as previously stated, a range improvement of 1 percent can be achieved for the VSCE by using the maximum duct burner reheat for this engine only above M = 0.8 rather than for the entire climb as was done in this report. In fact, private communications indicate that as much as 3 percent range improvement can be achieved relative to the maximum augmented climb cases if careful throttle scheduling is used during the climb. Further improvement are also expected in the structural weight fraction and perhaps in the high speed aerodynamics. The inlet design used in the present study is based on work done for the old U.S. Supersonic Transport effort and has not been optimized for the proposed variable-cycle engines. Increased attention to the inlet design could take advantage of the variable airflow characteristics of the variable-cycle engine to improve the low speed noise and transonic acceleration characteristics of these configurations.

CONCLUSIONS

An examination of the range potential of three candidate variable-cycle engines proposed for a second generation supersonic cruise transport was undertaken to determine the possible improvements in performance and to identify areas which require additional effort. This report is a status report on this effort. The three variable-cycle engines are descriptively designated as the Variable Stream Control Engine, the Rear Valve Engine, and the Double Bypass Engine.

The aircraft configuration chosen for the study had an arrow-wing planform with four engines mounted in separate pods beneath the wing. The takeoff gross weight and payload were fixed and the engine size and wing area were varied to achieve maximum range within certain operational restraints. The primary mission was a Mach number 2.6 hot day all - supersonic cruise; however the effects of a 1111-km (600 n.mi.) subsonic cruise element at

either the departure or arrival portion of the flight was considered. To determine the effects of noise regulations upon range, the maximum range was calculated for engines sized first without any noise restraint, then to satisfy the noise criteria but without the use of any form of suppression, and, last, to satisfy the noise regulation using annular/coannular noise relief.

For this latter case, the effect of relaxing certain of the operational restraints (for example takeoff field length and climb cruise thrust margin) was also studied. Sensitivities to changes in the operating weight empty, the propulsion system weight, the supersonic cruise SFC, the entire mission SFC, the supersonic cruise L/D and the entire mission L/D were also determined.

For the completely unrestrained cases (the "eye" of the thumbprint), the VSCE had a range of 7532 km (4067 n.mi.), the RVE had 7908 km (4270 n.mi.) and the DBE had a range of 6687 km (3611 n.mi.).

For engines sized to meet the noise limit with suppression, all engines had a range reduction of approximately 11 percent relative to their maximum unconstrained range.

If the takeoff field length restraint is changed from 3200 m (10500 ft) to 3810 m (12500 ft) the range of the VSCE increases by about 5 percent for the 108 EPNdB with suppression case while the RVE and DBE have smaller range improvements because of the climb excess thrust restraint. If the climb cruise excess thrust restrictions are also removed, the range of the RVE and DBE increase by about 6 percent relative to the 3200 m takeoff field length 108 EPNdB with suppression case.

For the 108 EPNdB with suppression case, the sensitivities for each of the engines are similar with the operating weight empty having the largest effect on range.

The calculated ranges reflect the stated assumptions and represent the current status of the in-house studies. Continuing work in the areas of low speed aerodynamics, noise reduction, structural efficiency and supersonic cruise efficiency promise to enable the designer to approach the ranges at the eye of the thumbprint as well as improving the ranges quoted for these maximum points.

REFERENCES

1. Nichols, M. R.; Keith, A. L.; and Foss, W. E.: "The Second Generation Supersonic Transport, Vehicle Technology for Civil Aviation - The Seventies and Beyond". NASA SP-292, November 1971.

2. Swan, W. C.; and Klees, G. W.: "Prospects for Variable-Cycle Engines". JANNAF/AIAA/SAE Paper CPI-228, November 1972.

3. Kless, G. W.; and Welliver, A. D.: "Variable-Cycle Engines for the Second Generation SST". SAE Paper 750630. Air Transportation Meeting, May 1975.

4. Willis, E.: "Variable-Cycle Engines for Supersonic Cruise Aircraft". 48th Propulsion and Energetics Panel Meeting, AGARD, September 1976.

5. Boxer, E.; Morris, S. J.; and Foss, W. E.: "Assessment of Variable-Cycle Engines for Supersonic Transports". 48th Propulsion and Energetics Panel Meeting, AGARD, September 1976.

6. Howlett, R. A.; and Kozlowski, H.: "Variable-Cycle Engines for Advanced Supersonic Transports". SAE Paper 751086, National Aerospace Engineering and Manufacturing Meeting, November 1975.

7. Byrd, K. F.; Oiler, T. L.; and Lichtman, E. A.: "Military High Mach Exhaust System Philosophy". JANNAF/AIAA/SAE 8th Propulsion Joint Specialists Conference, November 1972.

8. Stringas, E. J.; and Aver, H.: "In-Flight Noise Suppression Studies". Report No. CWR 300-69, Curtiss-Wright Corporation , June 1959.

9. Allan, R. D.: "Advanced Supersonic Propulsion System Technology Study, Phase II". NASA CR-134913, December 1975.

10. Baber, H. T.; and Swanson, E. E.: "Advanced Supersonic Technology Concept AST-100 Characteristics Developed in a Baseline-Update Study". NASA TM X-72815, January 1976.

11. Trans World Airline Staff: "An Airlines View of Reserve Fuel Requirements for the Supersonic Transport". LR-26133 Lockheed-California Co., Burbank, CA, September 19, 1973.

12. Fetterman, D.: "Preliminary Sizing and Performance Evaluation of Supersonic Cruise Aircraft". NASA TM X-73936, November 1976.

13. Smeltzer, D. B.; and Sorenson, N. E.: "Test of a Mixed Compression Axisymmetric Inlet With Large Transonic Mass Flow at Mach Number 0.6 to 2.65". NASA TN D-6971, December 1972.

14. Smeltzer, D. B.; and Sorenson, N. E.: "Analytic and Experimental Performance of Two Isentropic Axisymmetric Inlets at Mach Number 0.8 to 2.65". NASA TN D-7302, June 1973.

15. Tjonneland, E.: "The Design, Development, and Testing of a Supersonic Transport Intake System". AGARD-CP-91-71, 1971.

16. Stone, J. R.: "Iterim Prediction Method for Jet Noise". NASA TM X-71618, Lewis Research Center.

APPENDIX A

AERODYNAMIC DATA

The airplane aerodynamic performance data were obtained from a series of wind tunnel test and analytical computations. As presented in this appendix engine cowl pressure and skin friction drag were incorporated in the airplane aerodynamics. The inlet bleed, bypass, spillage and nozzle boattail drag have been charged to the engine net thrust to define the installed net thrust and specific fuel consumption (SFC). The aerodynamic data was scaled for variations in engine size and wing area (or wing loading) as described in reference 12.

The high speed trimmed drag polars are shown in figure A1. The drag coefficients obtained from this curve must be corrected for the environmental control system drag (figure A2) as well as for any variation in wing loading or engine cowl size. The data shown in figure A1 is for a wing loading of 415 kg/m^2 (85 lbm/ft^2) and excludes propulsion and environmental control system drags.

The low speed high lift aerodynamics must include the effects of flaps and of ground effects. The low speed configuration used in the present report is currently under review, however, it will be covered here for completeness. This information is based on unpublished data. The trimmed low speed lift coefficients (C_L) as a function of aircraft angle of attack for both the in ground effect and the out of ground effect for various flap angles are shown in figures A3 and A4. The in ground effect drag polars (C_D versus C_L) for various flap settings are shown in figure A5. The out of ground effect drag polars are shown in figure A6. All of the drag coefficients (C_D) are trimmed and include a ΔC_D due to the landing gear of 0.00849. In all cases the lift and drag coefficients are for a wing area of 785 sq. m. (8447 sq. ft.). Finally, the low speed trimmed lift drag ratio as a function of C_L is shown in figure A7. In this figure, the landing gear drag is included and the aircraft is assumed to be out of ground effects.

APPENDIX B

NOISE PREDICTION TECHNIQUES

This appendix presents a discussion of the calculation of the takeoff profile, the engine noise prediction methodology, and selection of the engine size used in this study. Also included is a typical study result for the case with the VSCE engine with no coannular suppression.

For a particular engine size and engine throttle setting, there isan engine thrust schedule as a function of velocity and altitude which is defined as a thrust table. This thrust table is employed in a takeoff program to define a takeoff profile which includes a time history of the aircraft's downrange distance, altitude, velocity, flight path angle, angle of attack, and engine thrust level. The takeoff data is then employed to ascertain the time-history of the observed perceived noise levels and the corresponding effective perceived noise levels (EPNL) at the observer locations.

Takeoff Profile

The takeoff noise levels are dependent on the takeoff profile which is presented in figure B1. Also shown on the figure are the two FAR 36 noise measurement points. The figure shows the takeoff field length from brake release to the 10.67 m (35 ft) obstacle is 3810 m (12,500 ft), and the thrust cutback point is at a downrange distance of 5944 m (19,500 ft). The minimum cutback altitude shown on the figure is set at 213 m (700 ft) except when the airframe noise exceeds 108 db at the centerline noise measurement station, in which case the cutback altitude is increased to reduce the airframe noise level. The landing gear is assumed to be fully retracted eight seconds after lift-off.

For this study, the low speed drag polars presented in Appendix A were employed and the gross takeoff weight (GTOW) was maintained at 325,678 kg (718,000 lbs. mass) independent of engine weight. This was done by trading fuel weight for engine weight. Prior to cutback, the wing trailing flaps are set at 20 degrees to minimize the sideline noise levels during takeoff as shown in reference 10. After cutback, the flaps are retracted to 5 degrees to reduce the required engine thrust level and thus the centerline noise levels.

To minimize the noise level at the centerline measurement point (fig. B1), the thrust level after cutback must be minimized. In accordance with FAR 36, the minimum thrust after cutback is that thrust required to maintain level flight at constant speed with one engine out. Thus, as the aircraft L/D increases, the thrust level after cutback can be reduced. Appendix A shows that for the present configuration at cutback, over the C_L range of operation (0.5 ± 0.15), the lower the C_L, the higher the L/D. Increasing

the aircraft velocity reduces both the C_L and the thrust level after cutback, and thus the noise level at the centerline measurement can be minimized.

The aircraft velocity at cutback can be increased by reducing the rate of climb and using the available thrust at the takeoff power setting to accelerate the aircraft. The aircraft takeoff profile is forced through a cutback point at the minimum cutback altitude which is normally 213 m (700 ft). However, as the aircraft velocity increases, the airframe noise level at the centerline measurement point increases and may exceed 108 db. For this case, the climb gradient prior to thrust cutback is increased and the cutback altitude is increased until the airframe noise level is equal to 108 db. The airframe noise prediction method is presented in reference 10. The noise levels at the measurement points are integrated time histories of the observed noise levels called effective perceived noise level (EPNL). Because the engine source noise level prior to thrust cutback is greater than after thrust cutback, it is necessary to have the thrust cutback occur prior to the time the aircraft passes directly over the centerline measurement point, which is 6486 m (21,280 ft) from brake release as shown in figure B1. The optimum cutback downrange distance was found to be 5944 m (19,500 ft) from brake release as shown in figure B1.

Engine Noise Prediction Method

Prediction of aircraft engine noise at ground observer stations is dependent on the engine exhaust nozzle flow characteristics, the aircraft velocity and the aircraft takeoff flight profile. The engine exhaust jet flow characteristics include exhaust jet area, nozzle velocity, exhaust jet density, and exhaust jet total temperature. In accordance with FAR 36 all takeoff performance characteristics are evaluated on a std $+10^{\circ}$ C day at 70 percent humidity.

The takeoff profile was divided into nine segments and the average engine exhaust flow characteristics, aircraft velocity, and altitude were calculated separately for each segment. These average properties were then employed to obtain the variation of engine source noise sound pressure level (SPL) over a range of frequency and directivity angles at a radius of 45.7 m (150 ft) from the center of the exit nozzle plane by using techniques described in reference 16.

The source noise SPL's are extrapolated from the source noise distance to the observer distance using the FAR 36 correction techniques. These include effects of spherical divergence, atmospheric attenuation, extra ground attenuation, ground reflection, and multi-engine shielding effects.

As the aircraft travels along the flight path, both the distance and the directivity angle between the aircraft and the observer vary. Thus, at a particular time, the variation of SPL with frequency at the observer station is computed. These SPL's are then added logarithmically to obtain a perceived noise level (PNL) at the observer station. As the aircraft approaches the observer location and passes by the observer location, the perceived noise

level increases to a maximum level (PNL_{MAX}) and then as the aircraft travels away from the observer, the PNL decreases again. The effective perceived noise level is obtained by integrating the PNL's over the time that the PNL first reaches 10 db below the maximum PNL until the time the PNL last reaches 10 db less than the maximum PNL. This integrated PNL-time level is then divided by a time interval of 10 seconds to obtain the effective perceived noise level (EPNL) in accordance with FAR 36.

Engine Size Selection

Each takeoff time history profile was derived from a particular thrust table which consists of 30 thrust points corresponding to ten velocities ranging from 0 to 137 m/sec. (0 to 450 ft/sec) and three altitudes: 0, 610, 1219 m (0, 2000, and 4000 ft). The takeoff profile is divided into nine segments and the average engine thrust and aircraft velocity and altitude are determined for each segment. These parameters, together with an engine scale factor, are then used to compute the average exhaust gas jet flow properties for each segment and the corresponding takeoff noise levels. For these same average takeoff parameters and a different engine scale factor, the average computed jet flow properties will change and the corresponding takeoff noise levels will change. Thus, for each takeoff thrust table, the effect of engine scale factor on takeoff noise level can be evaluated.

Typical Study Results

Figure B2 shows the variation of sideline EPNL with engine scale factor for five takeoff thrust tables. These values are based on the described configuration with four VSCE advanced engine concepts. From figure B2, it can be seen that for each thrust table, as the engine scale factor (ESF) increases, the sideline EPNL decreases due to the reduced power setting and jet velocities. Also shown from figure B2, it can be seen that a particular engine scale factor, the sideline noise level increases as the takeoff thrust levels increase. This is due to the higher power setting and higher jet velocities associated with the higher thrust levels.

Figure B3 shows the variation in centerline noise level with ESF for five takeoff thrust tables. From figure B3, it can be seen that for a particular thrust table as the ESF increases, the centerline noise level decreases, again due to the reduction in jet velocity. Also from figure B3, it can be seen that for a fixed engine scale factor (ESF), the centerline noise level decreases as the takeoff thrust levels increase. This is due to higher cutback L/D's associated with the higher initial takeoff thrust levels as described in the takeoff profile section of this appendix. At these higher L/D's, the required thrust level at cutback is reduced and thus the jet velocities and noise levels at the centerline measurement point are reduced.

As previously stated for a particular SLTO thrust level and the corresponding thrust table, the variation of engine size on noise level can be obtained by varying engine power setting. Figures B2 and B3 show the variation of sideline and centerline noise levels with engine size (ESF) respectively for several SLTO thrust levels. From these figures it can be seen that for each SLTO thrust value, there is a minimum ESF which meets the FAR 36 noise limit of 108 db. Figure B4 shows the variation of engine scale factor with sea level takeoff thrust value for both the sideline and centerline noise levels of 108 db. From figure B4, it can be seen that the minimum ESF required to meet the FAR 36 limit of 108 db is 0.90. This corresponds to an installed sea level takeoff thrust level of 257,493 n (57,887 lbs) per engine and the corresponding jet exit flow rate is 347 kg/sec. (765 lbs/sec). For the four-engine aircraft, the installed T/W is 0.3222. Also from figure B4, it can be seen that the actual takeoff thrust level required to meet the 108 db limit is 213,059 n (47,900 lbs), which corresponds to an engine power setting of 0.827.

For the cases where annular/coannular noise suppression was used, the engine specific thrust was computed for each ESF and throttle setting, and figure B5 was used to generate new centerline and sideline noise levels for these suppressed cases. A trade similar to that demonstrated in figure B4 was then made to determine ESF for these suppressed noise levels.

APPENDIX C

PROPULSION SYSTEM DATA

The propulsion system drag was defined as the summation of all the individual component throttle dependent drags. The boattail drag for each engine was used as supplied by the engine manufacturers for an isolated nacelle.

The boattail drag and the inlet bleed, spillage, and bypass drags were included in the computed net thrust and installed engine specific fuel consumption. The skin friction and cowl drag was included in the airplane drag. The cowl skin friction drag was scaled with the engine, but the cowl interference drag was held constant as engine size was varied.

The inlet was sized at a Mach number of 2.62, hot day, at an altitude of 65,000 feet. An allowance of 2 percent excess airflow was made at the design point to furnish cowl ventilation and to allow for engine to engine airflow variations. The inlet used in this study was a product of the 1969 SST effort and has not been optimized to take advantage of the variable cycle engine feature. In particular, the high airflow requirements at takeoff for the variable cycle engines could force redesign of the auxiliary airflow inlet doors.

The ratio of propulsion system drag to dynamic pressure (D/q) at maximum dry power as a function of flight Mach number is presented in figures C1, C2, and C3 for the VSCE, the RVE, and the DBE, respectively. Note the large peak boattail drag and the existance of significant supersonic cruise boattail drag for the DBE.

The effect of reduced power operation at subsonic cruise (Mach number 0.9 in the stratosphere) is shown in figures C4, C5, and C6 for the VSCE, the RVE, and the DBE, respectively. In these figures, the inlet drag to dynamic pressure ratio is shown as a function of net thrust to maximum dry net thrust ratio. Here the DBE demonstrates no penalty for throttling while the VSCE and RVE both suffer small penalties at the indicated subsonic cruise thrust level.

TABLE I. ENGINE SPECIFICATIONS
(UNINSTALLED 8° C HOT DAY)

	VSCE		RVE		DBE		GE4 (Standard day)	
Mass flow rate, kg/sec (lbm/sec)	408.2	(900)	408.2	(900)	435.4/362.9	(960/800)	287.1	(633)
Engine weight, kg (lbm)	6168.4	(13600)	6230.9	(13870)	7279.6	(16050)	6006.5	(13243)
Bypass ratio	1.3		2.5		0.35		0.0	
Fan pressure ratio	3.3		5.8		2.7/4.0		——	
Overall engine pressure ratio	16:1		21:1		17.3:1		12.5:1	
Max turbine inlet temperature, °K (°F)	1811	(2800)	1811	(2800)	1811	(2800)	1522	(2280)
Max secondary burner temperature, °K (°F)	1644	(2500)	1311	(1900)	1311	(1900)	1944	(3040)
Take-off max thrust, N (lbf)	286656	(64443)	287742	(64687)	299365	(67300)	284686	(64000)
Take-off SFC, kg/hr/N (lbm/hr/lbf)	.1482	(1.4546)	.11051	(1.0838)	.1224	(1.20)	.1896	(1.86)
Subsonic cruise								
Flight Mach number	0.9		0.9		0.9		0.9	
Flight altitude, m (ft)	10999	(36089)	10999	(36089)	10668	(35000)	11018	(36150)
Max net thrust, N (lbf)	111303	(25022)	100489	(22591)	84030	(18891)	108553	(24404)
SFC at max net thrust, kg/hr/N (lbm/hr/lbf)	.15719	(1.5416)	.1256	(1.2319) (TJ)	.1469	(1.441)	.187	(1.851)
Bypass ratio at max net thrust	1.2077		3.1692		0.36		0.0	
Net thrust at min SFC, N (lbf)	48899	(10993)	50567	(11368)	52155	(11725)	33930	(7290)
Min SFC, kg/hr/N (lbm/hr/lbf)	.0885	(.8681)	.08773	(.86039) (TF)	.11117	(1.003)	.106	(1.078)
Supersonic cruise								
Flight Mach number	2.62		2.62		2.62		2.62	
Flight altitude, m (ft)	19812	(65000)	19812	(65000)	19812	(65000)	19812	(65000)
Max net thrust, N (lbf)	128771	(28949)	79858	(17953)	74920	(16843)	99195	(22300)
SFC at max net thrust, kg/hr/N (lbm/hr/lbf)	.1793	(1.7584)	.15185	(1.4891)	.1588	(1.557)	.2008	(1.97)
Bypass ratio	1.5485		3.9927		0.74		0.0	
Net thrust at min SFC, N (lbf)	57124	(12842)	62221	(13988)	44810	(10074)	47151	(10600)
Min SFC, kg/hr/N (lbm/hr/lbf)	.1422	(1.3947)	.15020	(1.4730)	.1435	(1.408)	.1468	(1.44)

TABLE II. MISSION ELEMENTS — ALL SUPERSONIC

(a) No Noise Restraints

	GE4		VSCE		RVE		DBE	
Aircraft description								
Nominal engine airflow, kg/sec (lbm/sec)	266.7	(588)	371.9	(820)	368.3	(812)	347.7	(768)
Propulsion system weight	.1014		.1026		.1035		.1193	
Thrust loading, N/kg (lbf/lbm)	3.24	(.33)	3.21	(.327)	3.19	(.325)	3.53	(.360)
Wing loading, kg/m^2 (lbm/ft^2)	415.0	(85)	415.0	(85)	402.8	(82.5)	422.4	(86.5)
Operating weight empty	.443		.444		.448		.457	
Payload weight	.085		.085		.085		.085	
Mission description								
Weight at end of take-off	.982		.984		.986		.985	
Climb Δ Fuel weight	.137		.105		.118		.143	
Δ Range, km (n.mi.)	561	(303)	393	(212)	846	(457)	1018	(547)
Start of cruise, Weight	.863		.895		.882		.857	
Altitude, m (ft)	17983	(59000)	18092	(59360)	18565	(60910)	17983	(59000)
Lift-drag ratio	8.96		9.09		9.16		8.96	
SFC, kg/hr/N (lbm/hr/lbf)	.1677	(1.645)	.1552	(1.522)	.1592	(1.561)	.1613	(1.582)
Thrust ratio	.594		.518		.904		.828	
End of cruise, Weight	.649		.636		.632		.643	
Range, km (n.mi.)	5041	(2722)	6162	(3327)	6397	(3451)	5617	(3033)
End of descent, Weight	.641		.627		.626		.637	
Range, (km (n.mi.)	5560	(3002)	6714	(3625)	6949	(3752)	6165	(3329)
Burned fuel weight	.359		.373		.374		.363	
Total reserve fuel weight	.113		.098		.093		.095	
Total fuel weight	.472		.471		.467		.458	
Reserve								
In route fuel reserve weight	.025		.026		.026		.025	
Missed approach fuel weight	.017		.013		.010		.012	
Cruise to alternate fuel weight	.045		.038		.036		.037	
SFC, kg/hr/N (lbm/hr/lbf)	.1353	(1.327)	.1192	(1.169)	.1209	(1.186)	.1142	(1.120)
Mach number	.65		.70		.65		.70	
Altitude, m (ft)	4724	(15500)	4724	(15500)	4724	(15500)	4724	(15500)
Thrust ratio	.212		.173		.192		.352	
Hold fuel weight	.026		.021		.021		.021	

Note: All weights expressed as fractions of aircraft take-off gross weight.

TABLE II. MISSION ELEMENTS — ALL SUPERSONIC (Continued)

(b) 103 EPNdB, no Suppression

	GE4		VSCE		RVE		DBE	
Aircraft description								
Nominal engine airflow, kg/sec (lbm/sec)	401.9	(886.1)	388.7	(856.9)	417.0	(919.4)	377.4	(832.0)
Propulsion system weight	.1646		.1077		.1187		.1359	
Thrust loading, N/kg (lbf/lbm)	4.87	(.497)	3.35	(.342)	3.61	(.368)	3.83	(.390)
Wing loading, kg/m^2 (lbm/ft^2)	361.3	(74.0)	415.0	(85.0)	402.8	(82.5)	410.1	(84.0)
Operating weight empty	.525		.449		.463		.478	
Payload weight	.085		.085		.085		.085	
Mission description								
Weight at end of take-off	.981		.984		.986		.986	
Climb Δ Fuel weight	.108		.103		.103		.128	
Δ Range, km (n.mi)	285	(154)	365	(197)	628	(339)	809	(437)
Start of cruise, Weight	.892		.897		.897		.872	
Altitude, m (ft)	18843	(61820)	18091	(59355)	18851	(61850)	17983	(59000)
Lift-drag ratio	8.904		9.073		9.099		8.981	
SFC, kg/hr/N (lbm/hr/lbf)	.1560	(1.530)	.1548	(1.518)	.1594	(1.563)	.1593	(1.562)
Thrust ratio	.472		.498		.856		.776	
End of cruise, Weight	.753		.643		.652		.666	
Range, km (n.mi)	3132	(1691)	6008	(3244)	5904	(3188)	5208	(2812)
End of descent, Weight	.743		.634		.645		.659	
Range, km (n.mi)	3647	(1969)	6562	(3543)	6463	(3490)	5758	(3109)
Burned fuel weight	.257		.366		.355		.341	
Total reserve fuel weight	.133		.100		.097		.096	
Total fuel weight	.390		.466		.452		.437	
Reserve								
In route fuel reserve weight	.018		.026		.025		.024	
Missed approach fuel weight	.028		.014		.011		.013	
Cruise to alternate fuel weight	.055		.038		.038		.038	
SFC, kg/hr/N (lbm/hr/lbf)	.1448	(1.420)	.1208	(1.185)	.1231	(1.207)	.1142	(1.120)
Mach number	.65		.70		.75		.70	
Altitude, m (ft)	4724	(15500)	4724	(15500)	4724	(22000)	4724	(15500)
Thrust ratio	.165		.167		.218		.352	
Hold fuel weight	.032		.022		.022		.021	

Note: All weights expressed as fractions of aircraft take-off gross weight

TABLE II. MISSION ELEMENTS — ALL SUPERSONIC (Concluded)

(c) 108 EPNdB, With Suppression

	GE4		VSCE		RVE		DBE	
Aircraft description								
Nominal engine airflow, kg/sec (lbm/sec)	316.7	(698.2)	371.9	(820.0)	375.6	(828.0)	352.3	(776.7)
Propulsion system weight	.1289		.1026		.1058		.1254	
Thrust loading, N/kg (lbf/lbm)	3.84	(.392)	3.21	(.327)	3.25	(.331)	3.57	(.364)
Wing loading, kg/m^2 (lbm/ft^2)	395.5	(81.0)	415.0	(85)	402.8	(82.5)	422.3	(86.5)
Operating weight empty	.477		.444		.450		.464	
Payload weight	.085		.085		.085		.085	
Mission description								
Weight at end of take-off	.982		.984		.986		.986	
Climb Δ Fuel weight	.120		.105		.115		.140	
Δ Range, km (n.mi)	407	(220)	393	(212)	79[illegible]	(431)	980	(529)
Start of cruise, Weight	.879		.895		.885		.860	
Altitude, m (ft)	17983	(59000)	18092	(59360)	18550	(60860)	17983	(59000)
Lift-drag ratio	8.816		9.09		9.15		8.96	
SFC, kg/hr/N (lbm/hr/lbf)	.1562	(1.532)	.1552	(1.522)	.1591	(1.5605)	.1610	(1.579)
Thrust ratio	.517		.518		.888		.821	
End of cruise, Weight	.692		.636		.635		.650	
Range, km (n.mi)	4304	(2324)	6162	(3327)	6321	(3413)	5465	(2951)
End of descent, Weight	.683		.627		.629		.644	
Range, km (n.mi)	4817	(2601)	6714	(3625)	6878	(3714)	6013	(3247)
Burned fuel weight	.317		.373		.371		.356	
Total reserve fuel weight	.121		.098		.094		.095	
Total fuel weight	.438		.471		.465		.451	
Reserve								
In route fuel reserve weight	.022		.026		.026		.025	
Missed approach fuel weight	.021		.013		.010		.012	
Cruise to alternate fuel weight	.049		.038		.037		.037	
SFC, kg/hr/N (lbm/hr/lbf)	.1392	(1.365)	.1192	(1.1688)	.1215	(1.1919)	.1142	(1.120)
Mach number	.65		.70		.65		.70	
Altitude, m (ft)	4724	(15500)	4724	(15500)	4724	(15500)	4724	(15500)
Thrust ratio	.192		.173		.189		.352	
Hold fuel weight	.029		.021		.021		.021	

Note: All weights expressed as fractions of aircraft take-off gross weight

TABLE III. MISSION ELEMENTS
600 NAUTICAL MILE SUBSONIC CRUISE — 108 EPNdB WITH SUPPRESSION

(a) Subsonic Cruise Departure

		GE4		VSCE		RVE		DBE	
Aircraft description									
Nominal engine airflow, kg/sec (lbm/sec)		316.7	(698.2)	371.9	(820.0)	375.6	(828.0)	352.3	(776.7)
Propulsion system weight		.1289		.1026		.1058		.1254	
Thrust loading, N/kg (lbf/lbm)		3.84	(.392)	3.21	(.327)	3.25	(.331)	3.57	(.364)
Wing loading, kg/m^2 (lbm/ft^2)		395.5	(81.0)	415.0	(85.0)	402.8	(82.5)	422.3	(86.5)
Operating weight empty		.477		.444		.450		.464	
Mission description									
Weight at end of take-off		.981		.984		.986		.986	
Start of subsonic cruise,	Weight	.954		.959		.965		.960	
	Altitude, m (ft)	6096	(20000)	6096	(20000)	6096	(20000)	6096	(20000)
	Lift-drag ratio	13.90		14.31		14.37		14.23	
	SFC, kg/hr/N (lbm/hr/lbf)	.1580	(1.549)	.1102	(1.081)	.1136	(1.114)	.1222	(1.198)
	Thrust ratio	.2443		.2750		.3000		.3650	
End of subsonic cruise,	Weight	.847		.884		.889		.878	
Start of supersonic cruise,	Weight	.783		.829		.821		.797	
	Altitude	18649	(61185)	18589	(60990)	19042	(62475)	18346	(60190)
	Lift-drag ratio	8.514		9.041		9.105		8.888	
	SFC, kg/hr/N (lbm/hr/lbf)	.1563	(1.532)	.1553	(1.523)	.1592	(1.561)	.1607	(1.576)
	Thrust ratio	.5328		.5224		.8965		.8143	
End of supersonic cruise,	Weight	.692		.636		.635		.650	
	Range, km (n.mi)	3458	(1867)	5932	(3203)	6071	(3278)	5182	(2798)
End of descent,	Weight	.683		.627		.629		.644	
Range, km (n.mi)		3971	(2144)	6486	(3502)	6626	(3578)	5730	(3094)
Total reserve fuel weight		.121		.098		.094		.095	
Total fuel weight		.438		.471		.465		.451	
Reserves									
In route fuel reserve weight		.022		.026		.026		.025	
Missed approached fuel weight		.021		.013		.010		.012	
Cruise to alterante fuel weight		.049		.038		.037		.037	
	SFC, kb/hr/N (lbm/hr/lbf)	.1392	(1.365)	.1192	(1.196)	.1215	(1.192)	.1142	(1.120)
	Mach number	.65		.70		.65		.70	
	Altitude, m (ft)	4724	(15500)	4724	(15500)	4724	(15500)	4724	(15500)
Hold fuel weight		.029		.021		.021		.021	

Note: All weights expressed as fractions of aircraft take-off gross weight.

TABLE III. MISSION ELEMENTS
600 NAUTICAL MILE SUBSONIC CRUISE — 108 EPNdB WITH SUPPRESSION (Concluded)

(b) Subsonic Cruise Arrival

		GE4		VSCE		RVE		DBE	
Aircraft description									
Nominal engine airflow, kg/sec (lbm/sec)		317.0	(698.9)	371.9	(820.0)	375.1	(827.0)	352.2	(776.5)
Propulsion system weight		.1289		.1026		.1058		.1254	
Thrust loading, N/kg (lbf/lbm)		3.84	(.392)	3.21	(.327)	3.25	(.331)	3.57	(.364)
Wing loading, kg/m^2 (lbm/ft^2)		395.5	(81.0)	415.0	(85.0)	402.8	(82.5)	422.3	(86.5)
Operating weight empty		.477		.444		.450		.464	
Mission description									
Weight at end of take-off		.981		.984		.986		.986	
Start of supersonic cruise,	Weight	.879		.895		.885		.860	
	Altitude, m (ft)	17983	(59000)	18092	(59360)	18548	(60855)	17983	(59000)
	Lift-drag ratio	8.841		9.088		9.152		8.962	
	SFC, kg/hr/N (lbm/hr/lbf)	.1560	(1.530)	.1552	(1.522)	.1592	(1.561)	.1610	(1.579)
	Thrust ratio	.530		.518		.888		.821	
End of supersonic cruise,	Weight	.779		.691		.692		.714	
	Range km (n.mi)	2393	(1292)	4767	(2574)	4897	(2644)	3971	(2144)
Start of subsonic cruise,	Weight	.775		.688		.690		.712	
	Altitude, m (ft)	9144	(30000)	9144	(30000)	9144	(30000)	9144	(30000)
	Lift-drag ratio	13.980		14.16		14.24		14.06	
	SFC, kg/hr/N (lbm/hr/lbf)	.1511	(1.482)	.1070	(1.049)	.1095	(1.074)	.1178	(1.155)
	Thrust ratio	.297		.304		.332		.418	
End of subsonic cruise,	Weight	.689		.634		.634		.650	
End of descent,	Weight	683		.627		.629		.644	
Range, km (n.mi)		4024	(2173)	6437	(3476)	6651	(3591)	5637	(3044)
Total reserve fuel weight		.121		.098		.094		.095	
Total fuel weight		.438		.471		.465		.451	
Reserves									
In route fuel reserve weight		.020		.026		.026		.025	
Missed approach fuel weight		.023		.013		.010		.012	
Cruise to alternate fuel weight		.049		.038		.037		.037	
	SFC, kg/hr/N (lbm/hr/lbf)	.1393	(1.366)	.1192	(1.169)	.1215	(1.192)	.1142	(1.120)
	Mach number	.65		.70		.65		.70	
	Altitude, m (ft)	4724	(15500)	4724	(15500)	4724	(15500)	4724	(15500)
Hold fuel weight		.029		.021		.021		.021	

Note: All weights expressed as fractions of aircraft take-off gross weight

TABLE IV. RANGE SUMMARY - ALL SUPERSONIC MISSION

Condition	Cruise Thrust Margin	Climb Thrust Margin	Field Length Restraint	GE4	VSCE	RVE	DBE
				RANGE, km. (n.mi)			
No Restraint	None	None	None	5971 (3224)	7532 (4067)	7908 (4270)	6687 (3611)
No Noise Restraint	1.1	1.2	(10500 ft)	5560 (3002)	6714 (3625)	6949 (3752)	6165 (3329)
108 EPNdB, No Suppression	1.1	1.2	(10500 ft)	3647 (1969)	6562 (3543)	6463 (3490)	5758 (3109)
108 EPNdB, With Suppression	1.1	1.2	(10500 ft)	4817 (2601)	6714 (3625)	6878 (3714)	6013 (3247)
108 EPNdB, With Suppression	1.1	1.2	(12500 ft)	N/A	7059 (3812)	6949 (3752)	6168 (3329)
108 EPNdB, With Suppression	None	None	(12500 ft)	N/A	7059 (3812)	7285 (3934)	6435 (3475)

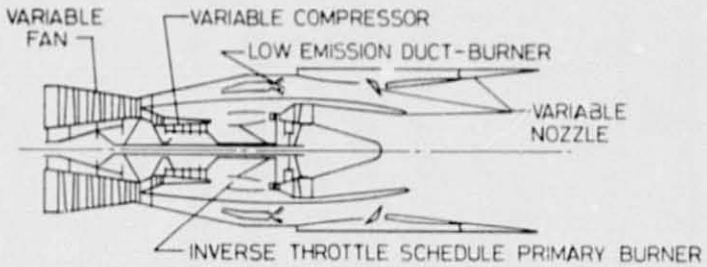

(a) Variable stream control engine (VSCE).

TWIN TURBOJET

DUCT BURNER ON

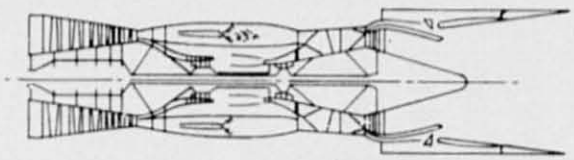

DUCT BURNER OFF

TURBOFAN

(b) Rear value engine (RVE).

TAKEOFF AND SUBSONIC OPERATION

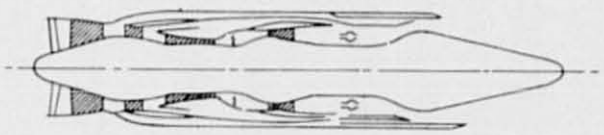

CLIMB AND SUPERSONIC CRUISE

(c) Double bypass engine (DBE).

Figure 1.- Variable cycle engines.

NOTE: DIMENSIONS SHOWN IN METERS WITH FEET IN PARENTHESIS

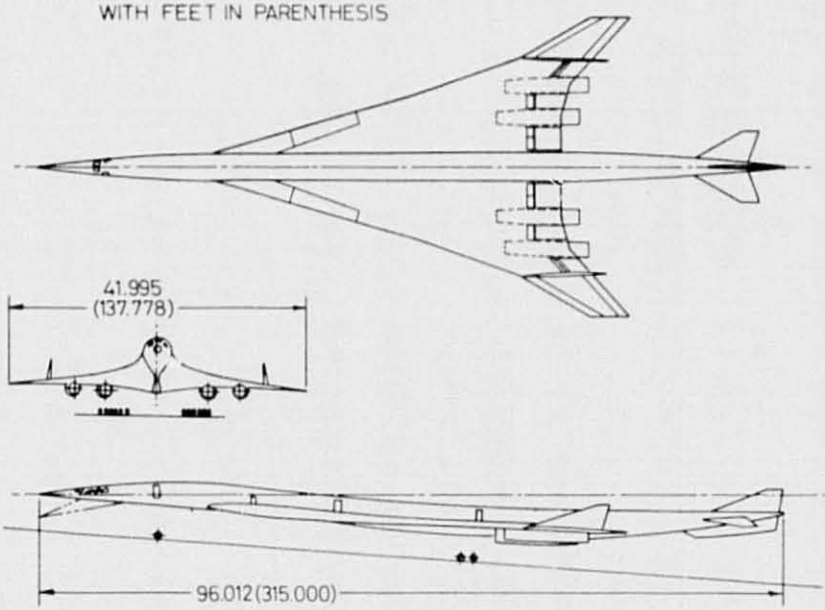

Figure 2.- General arrangement of the airplane.

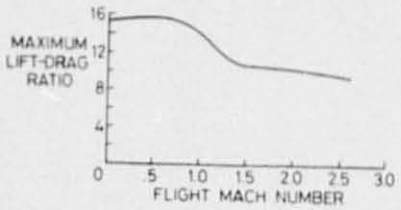

Figure 3.- Maximum lift-drag ratio.

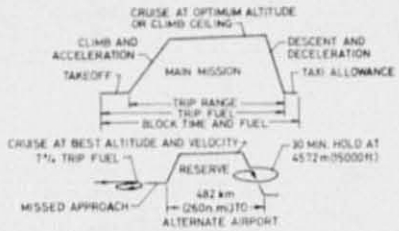

Figure 4.- Mission profiles/reserves.

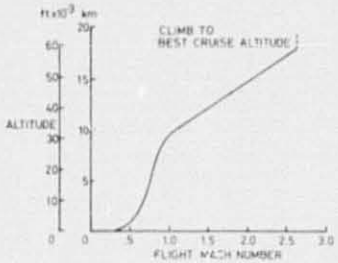

Figure 5.- Climb schedule.

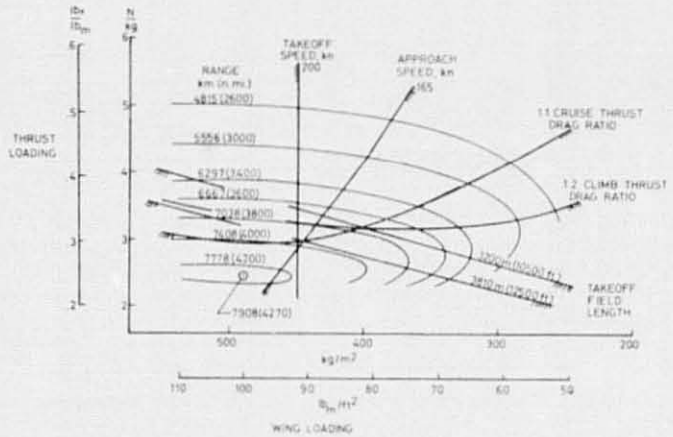

Figure 6.- Engine airplane range diagram for the RVE.

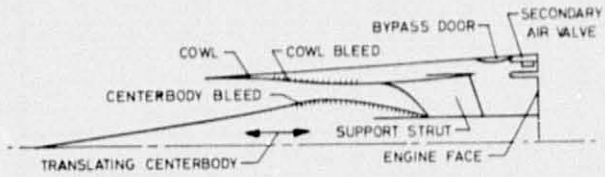

(a) Inlet schematic.

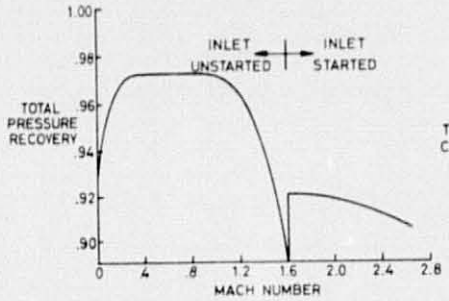

(b) Inlet pressure recovery.

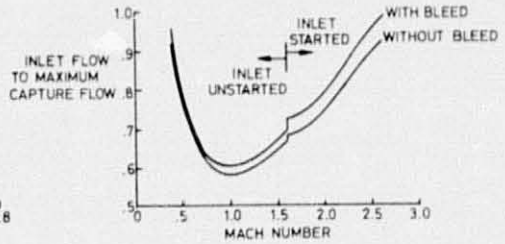

(c) Inlet airflow schedule.

Figure 7.- Inlet description

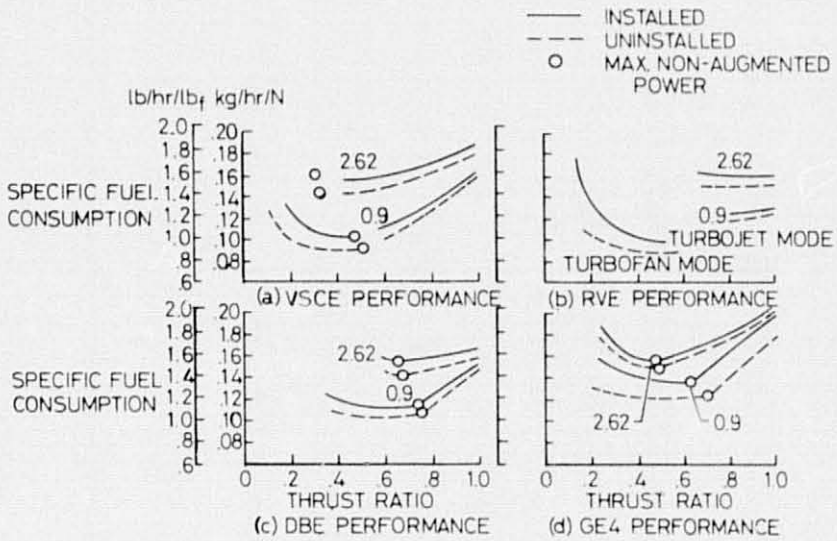

Figure 8.- Installed and uninstalled engine performance.

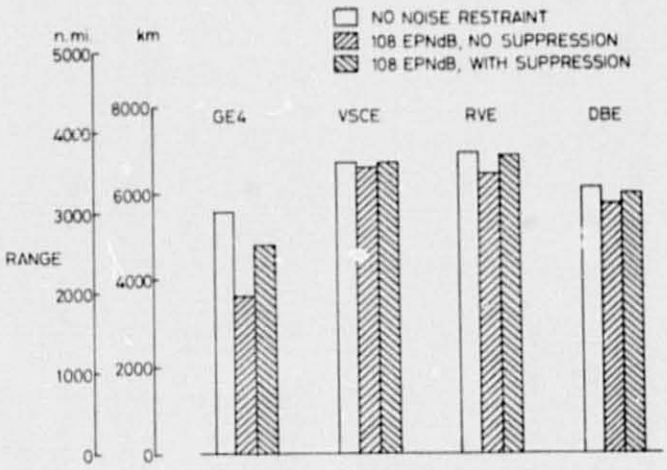

Figure 9.- Maximum range comparison for all supersonic mission.

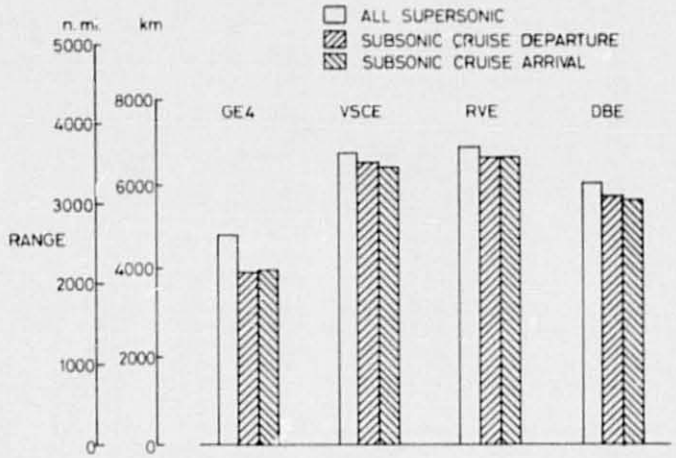

Figure 10.- Effect of subsonic element.

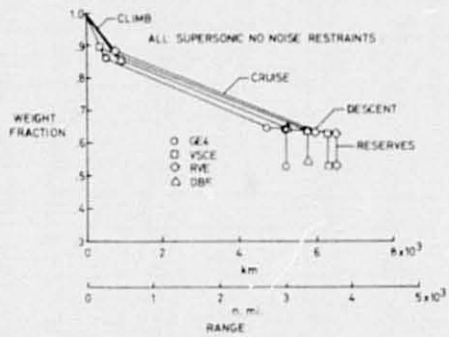

Figure 11.- Fuel usage versus range.

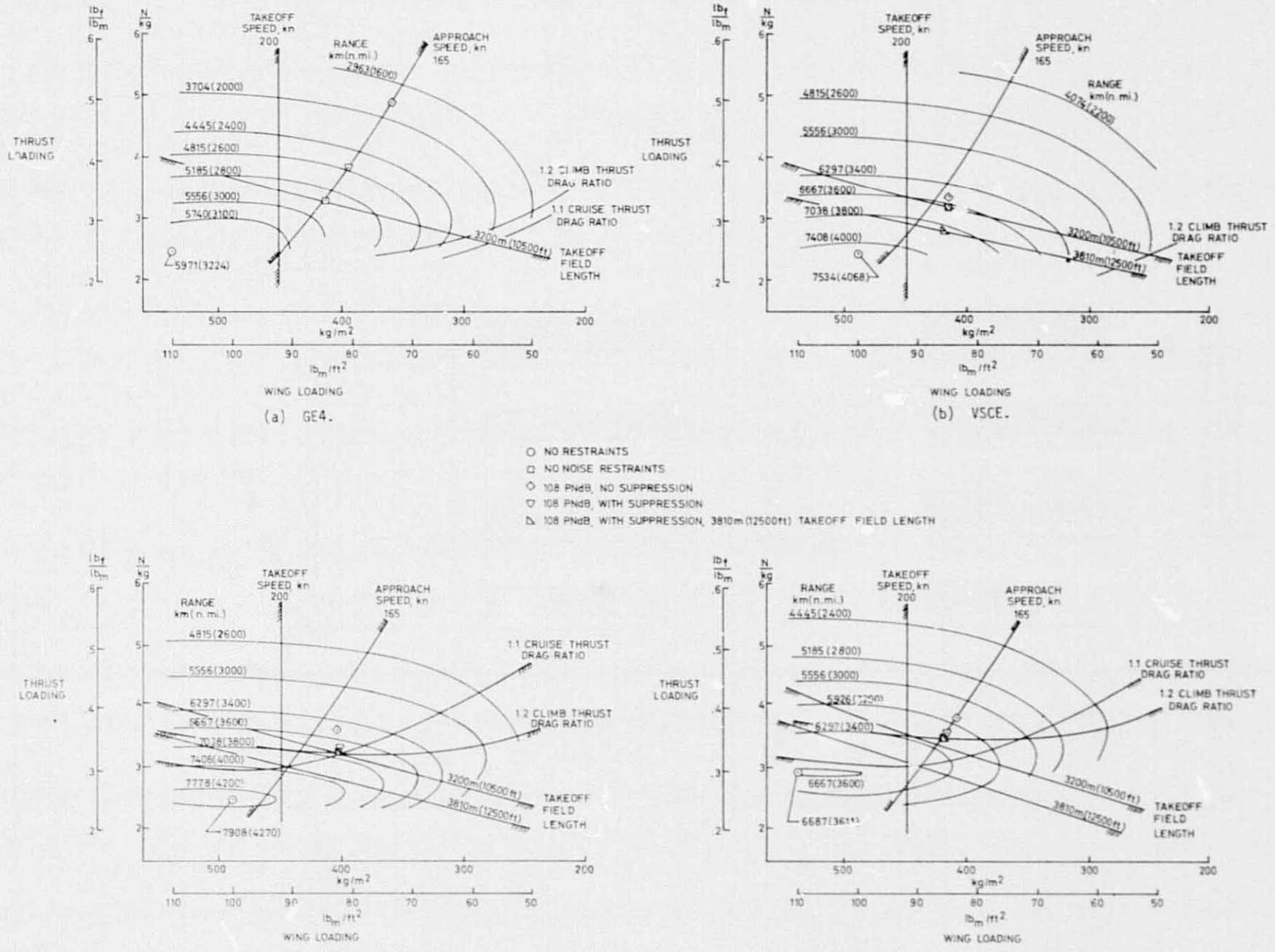

Figure 12.- Engine airplane range diagrams.

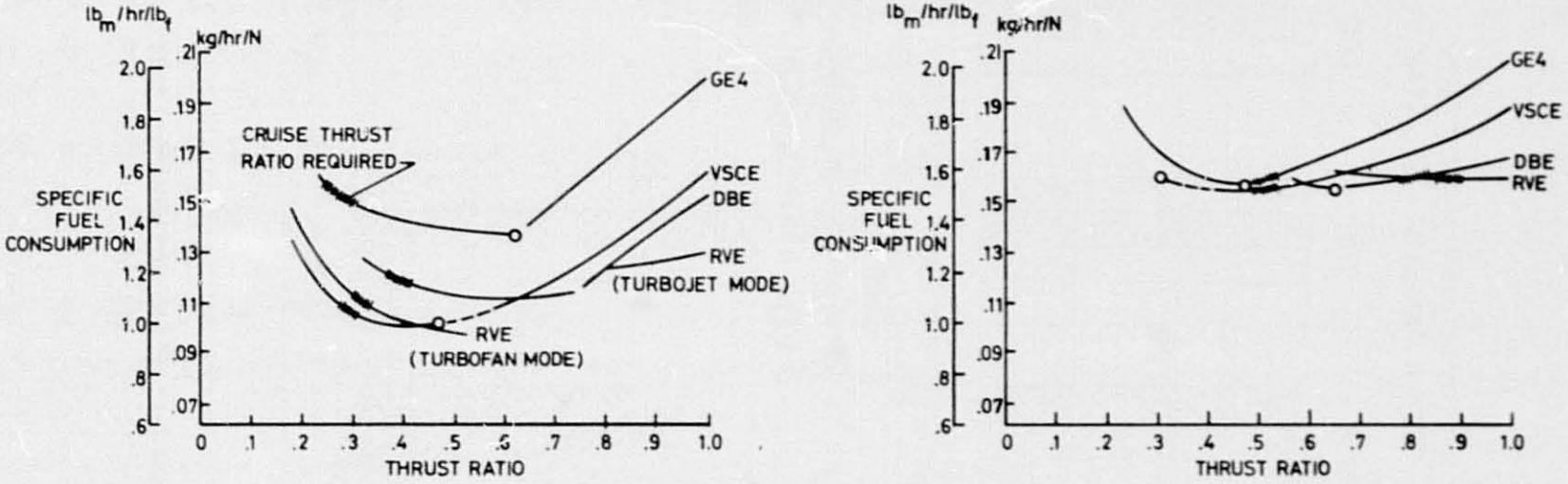

(a) Mach number = 0.9.

(b) Mach number = 2.62.

Figure 13.- Installed engine performance.

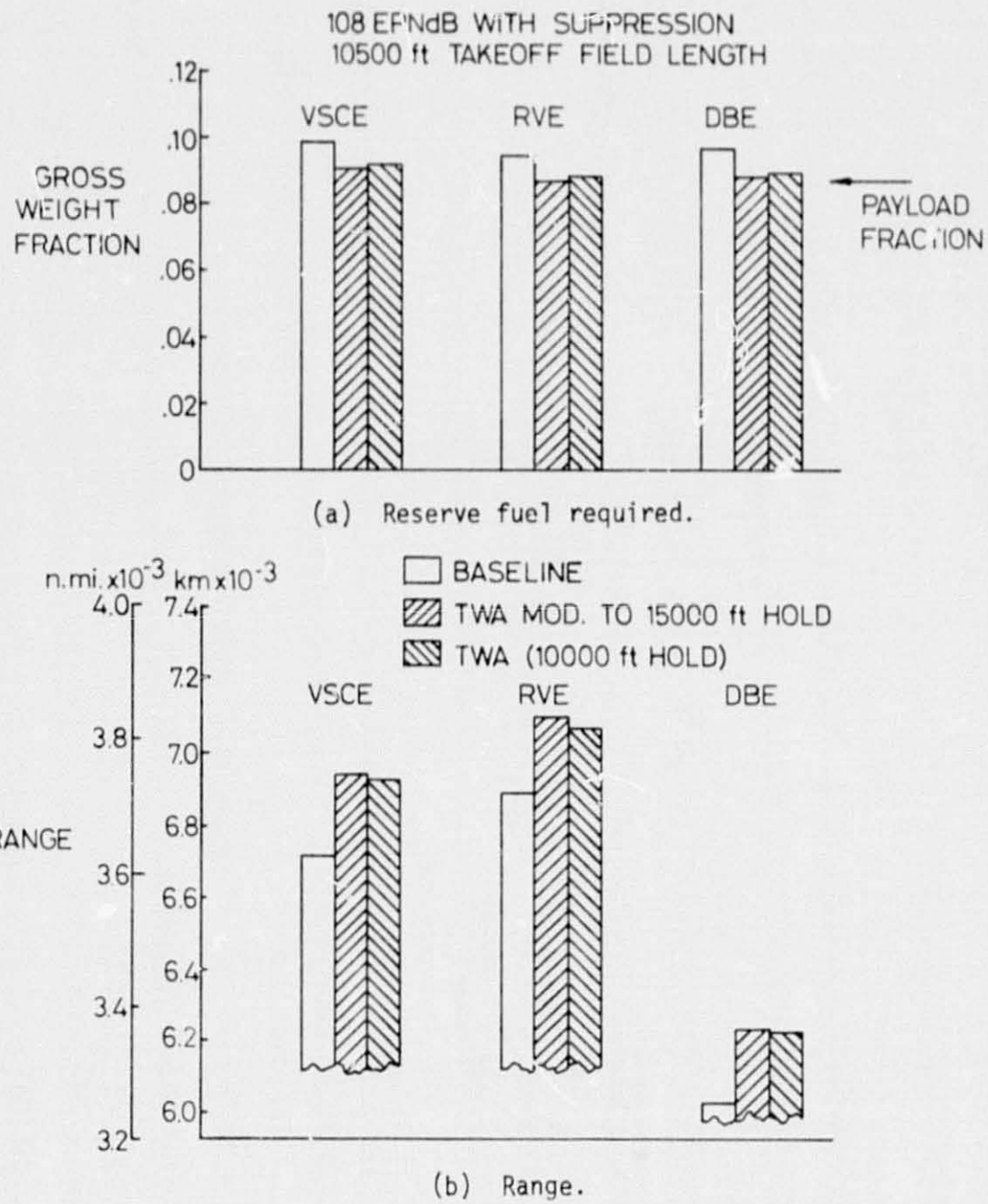

Figure 14.- Effect of reserve requirements on fuel reserve and range.

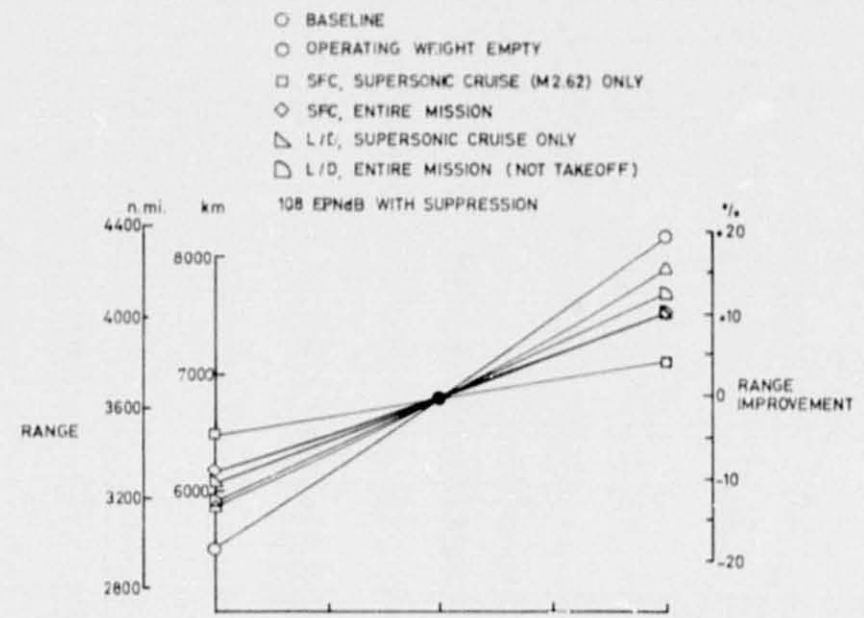

(a) VSCE.

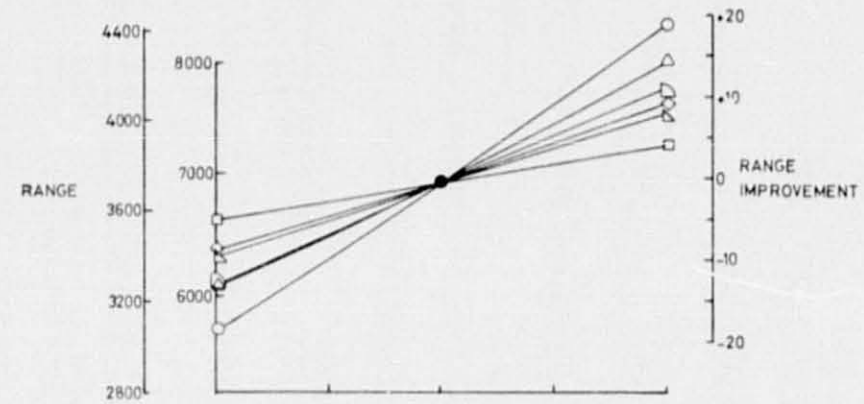

(b) RVE.

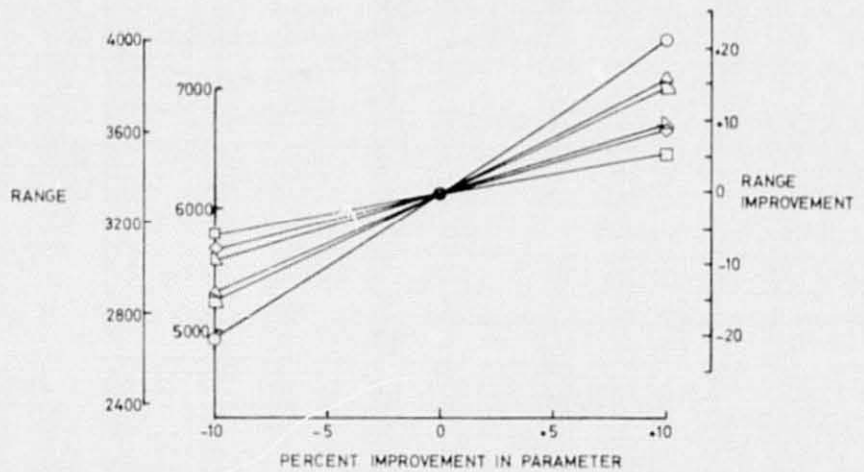

(c) DBE.

Figure 15. Range sensitivity.

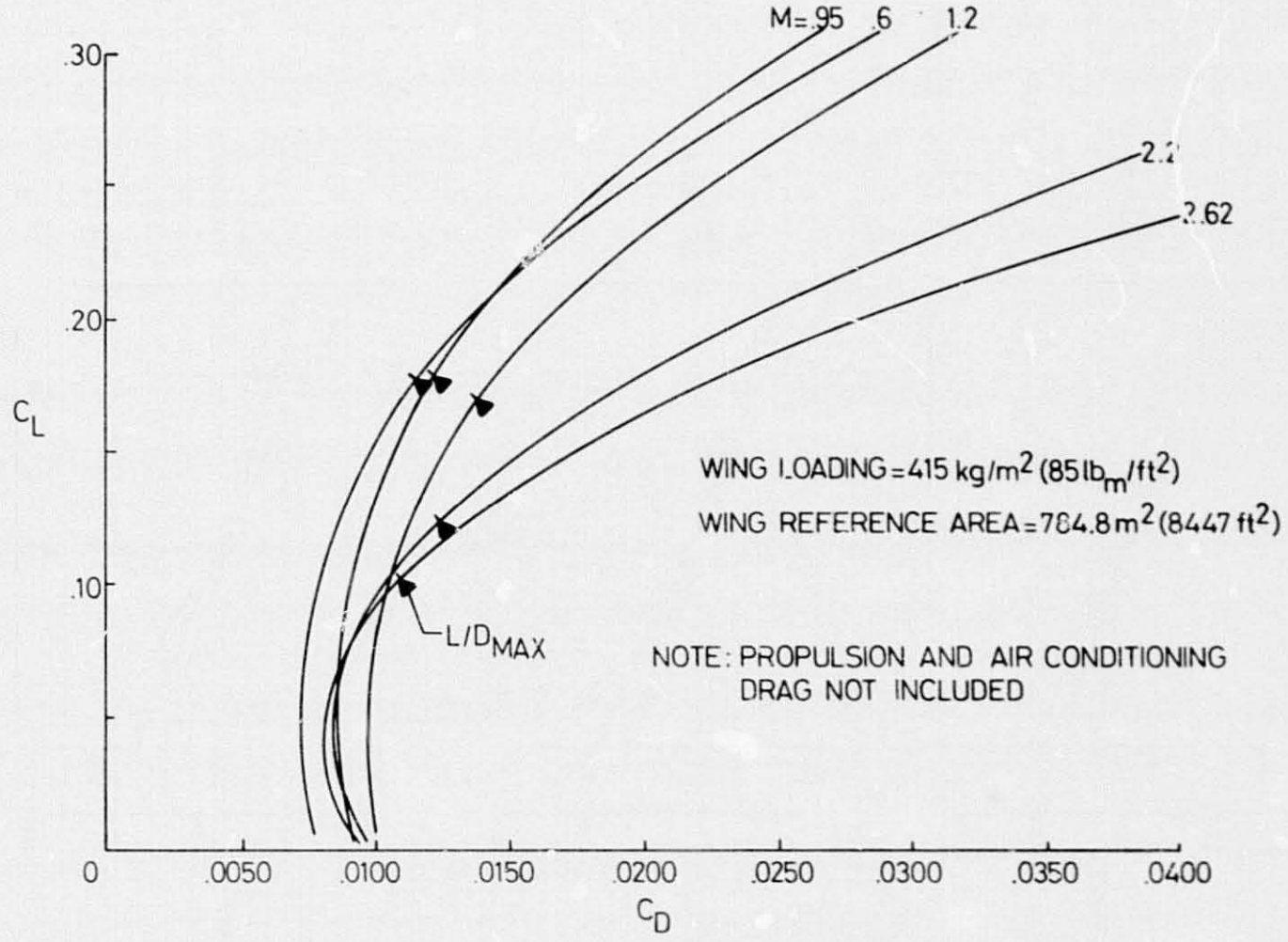

Figure A1.- High speed drag polars.

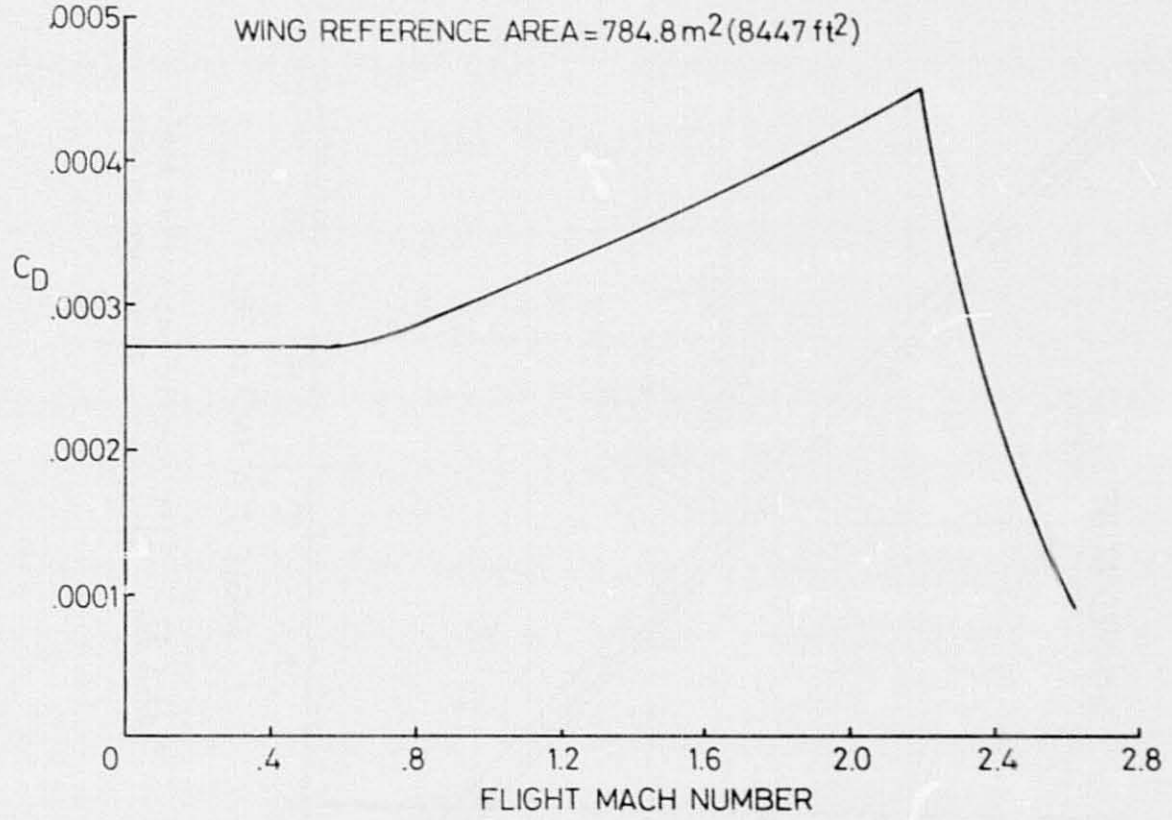

Figure A2.- Environmental control system drag.

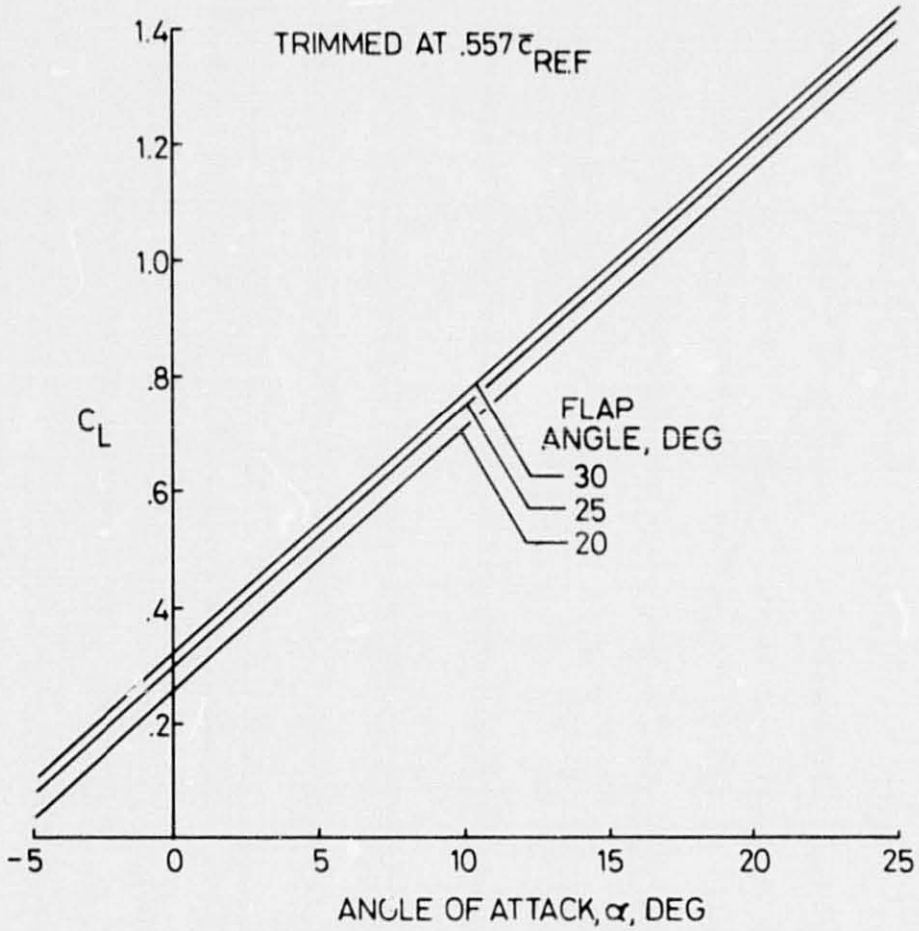

Figure A3.- Lift coefficient versus angle of attack - In ground effect.

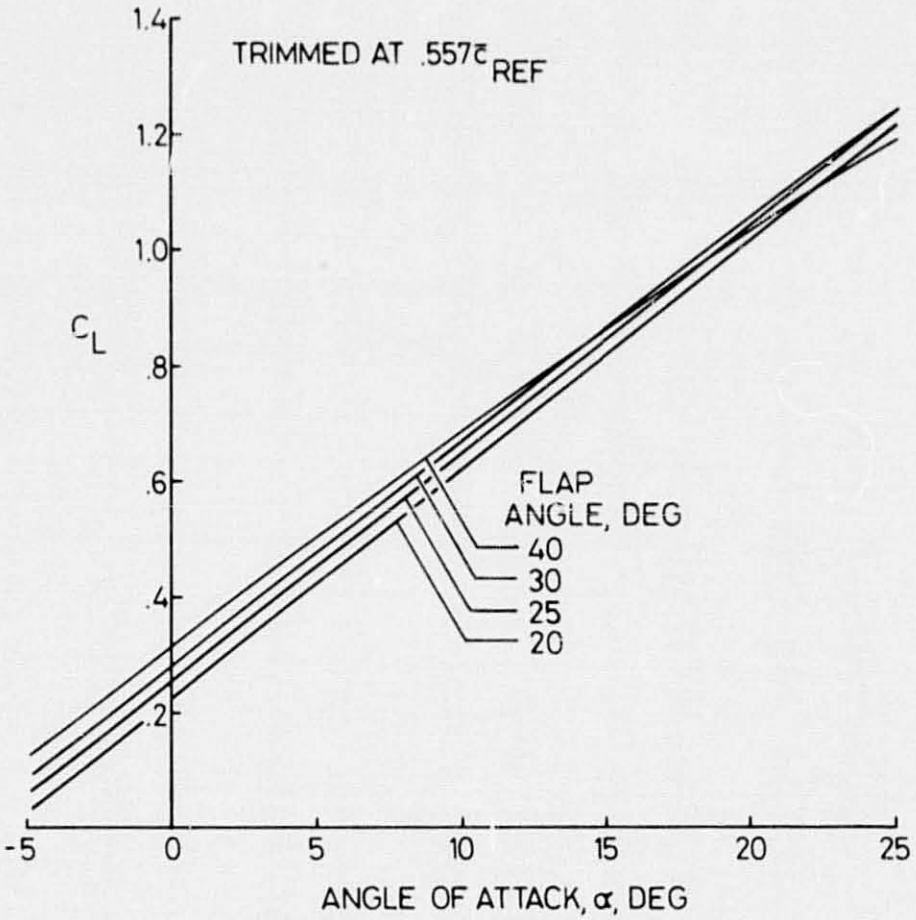

Figure A4.- Lift coefficient versus angle of attack - Out of ground effect.

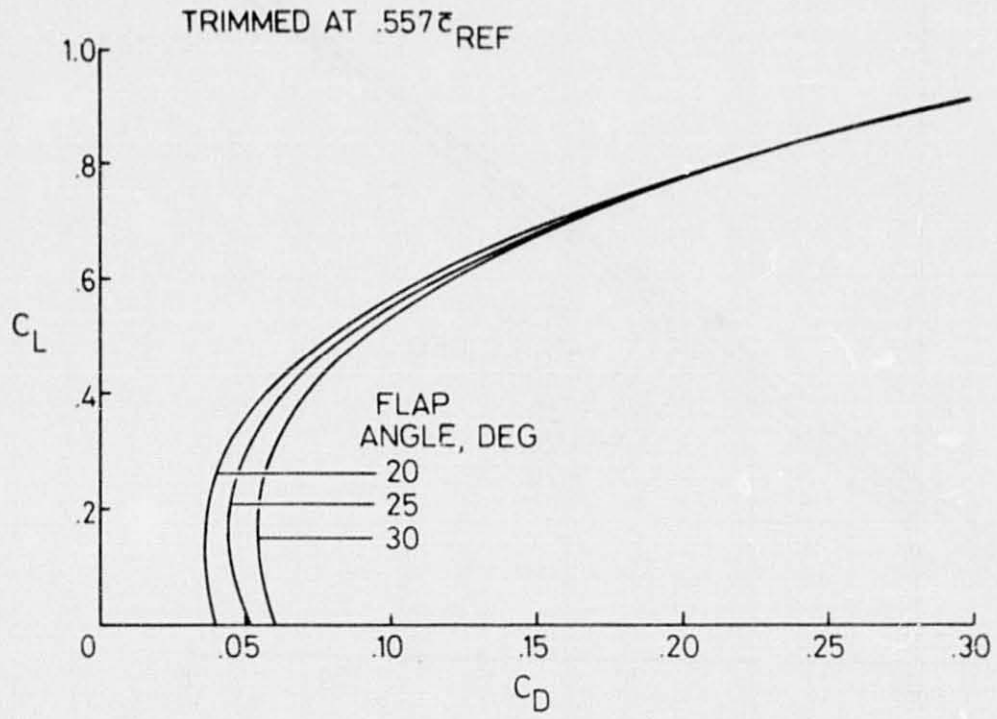

Figure A5.- Low speed drag polars - In ground effect with landing gear down.

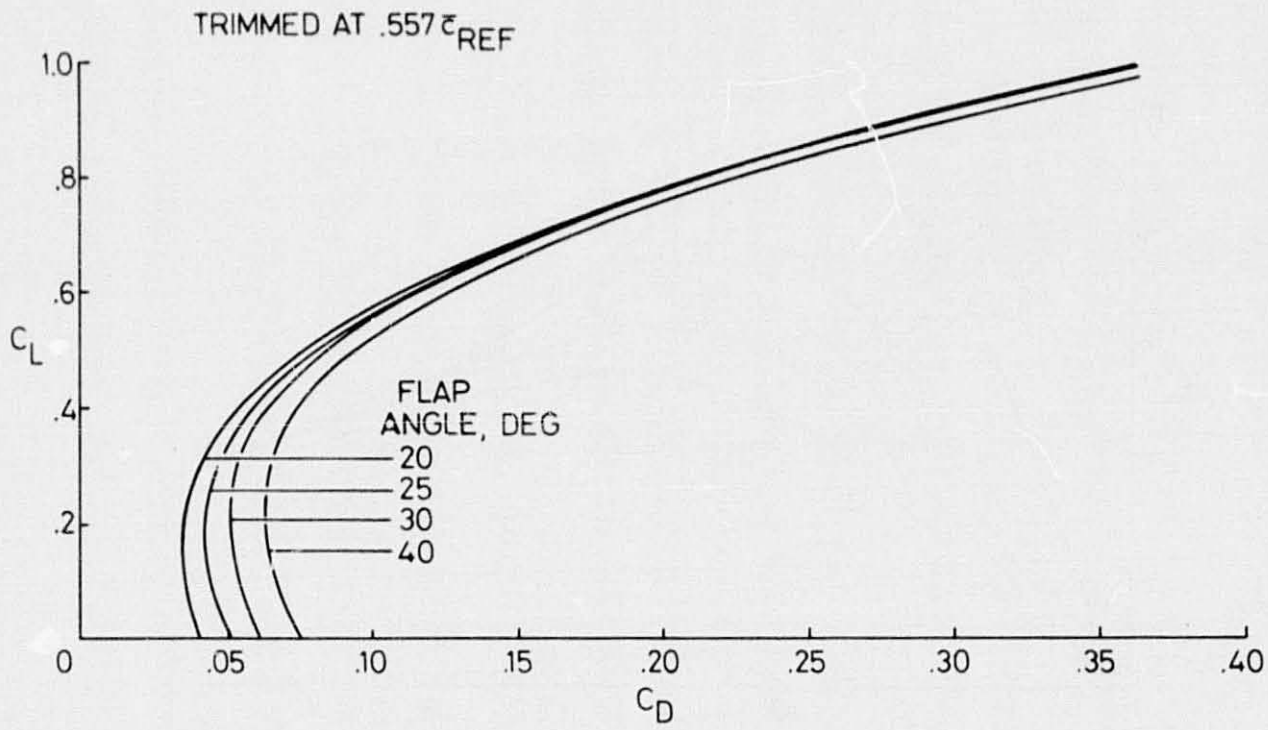

Figure A6.- Low speed drag polar - Out of ground effect with landing gear down.

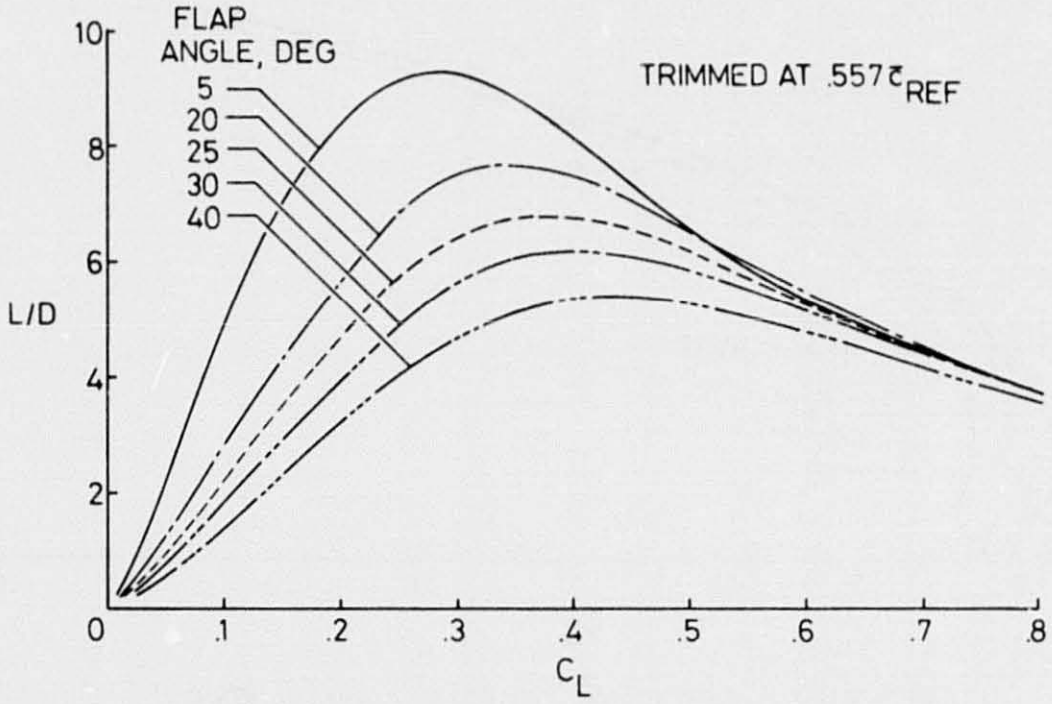

Figure A7.- Low speed lift-drag ratio.

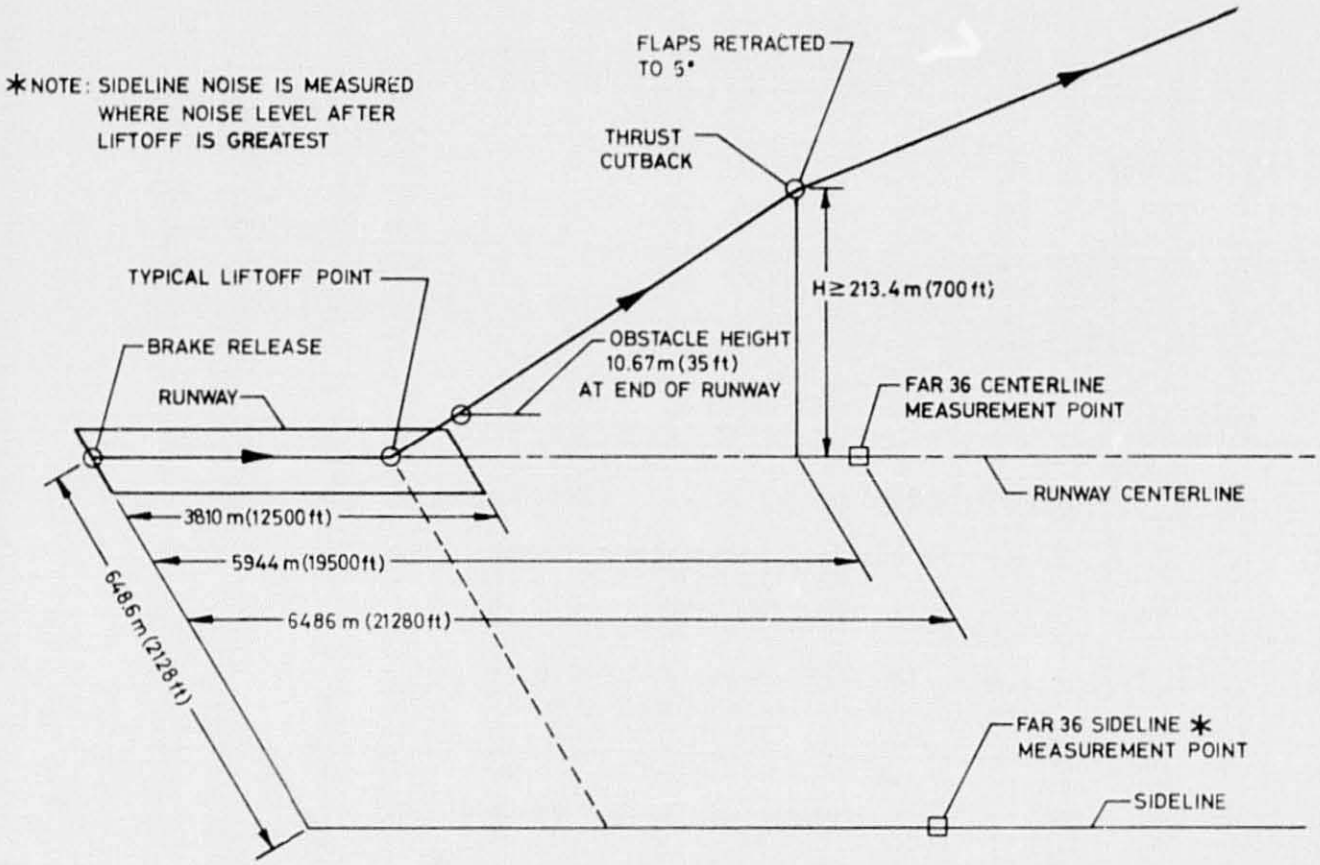

Figure B1.- Typical take-off trajectory.

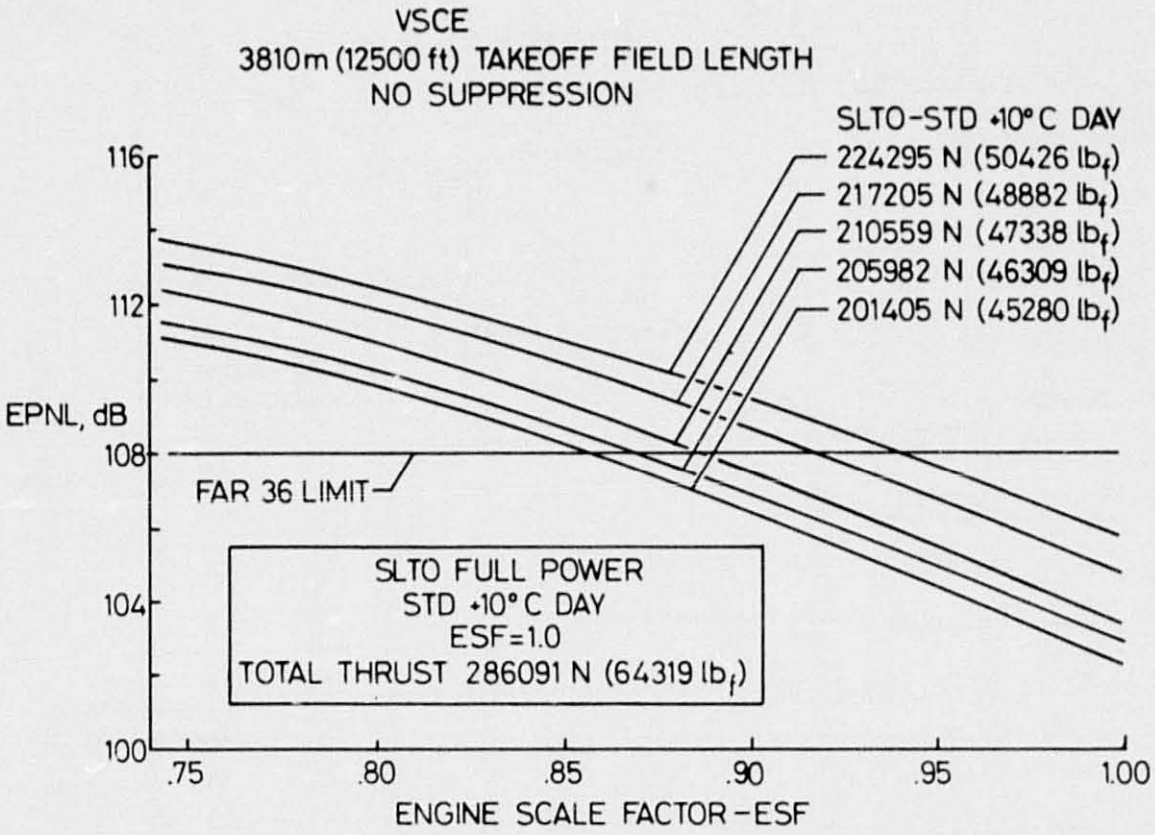

Figure B2.- Variation of sideline EPNL with engine scale factor.

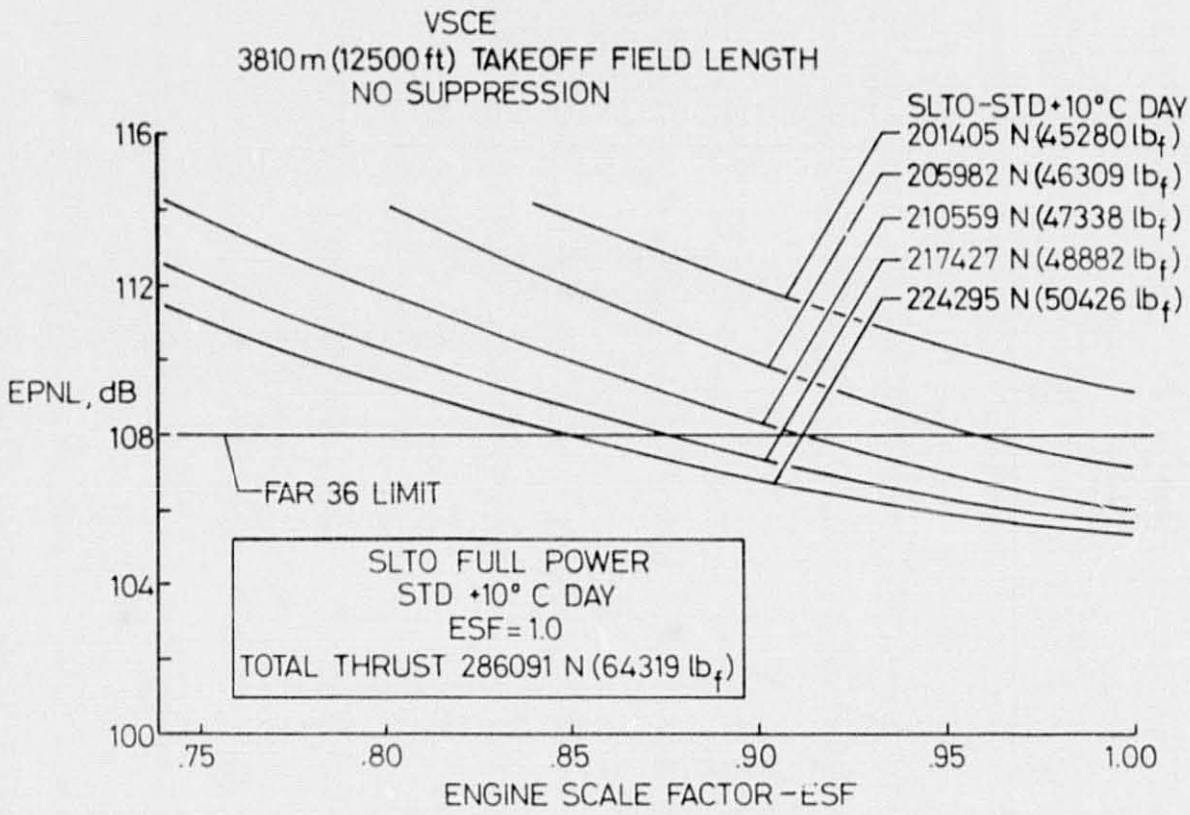

Figure B3.- Variation of centerline EPNL with engine scale factor.

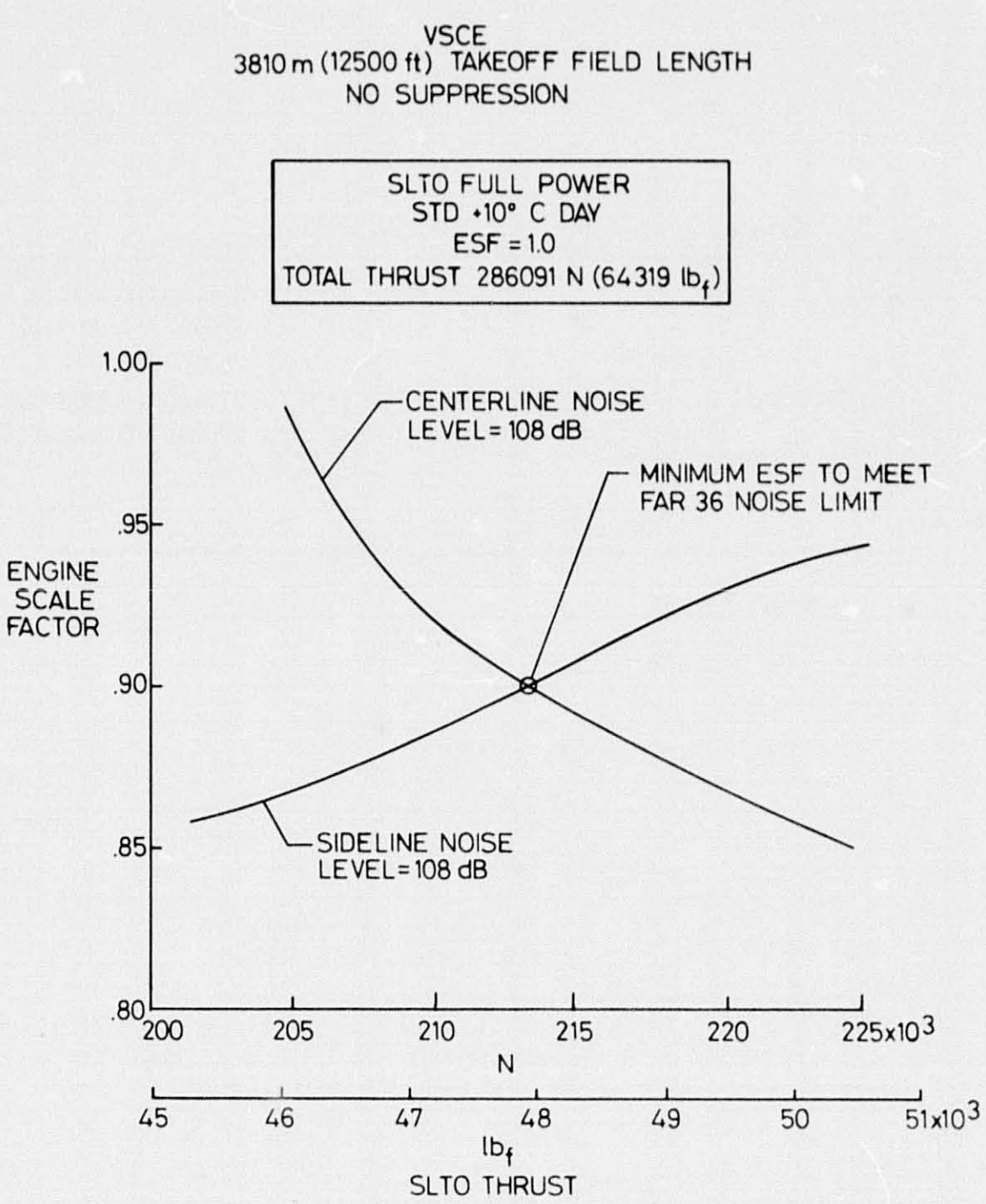

Figure B4.- Variation of engine scale factor with take-off thrust.

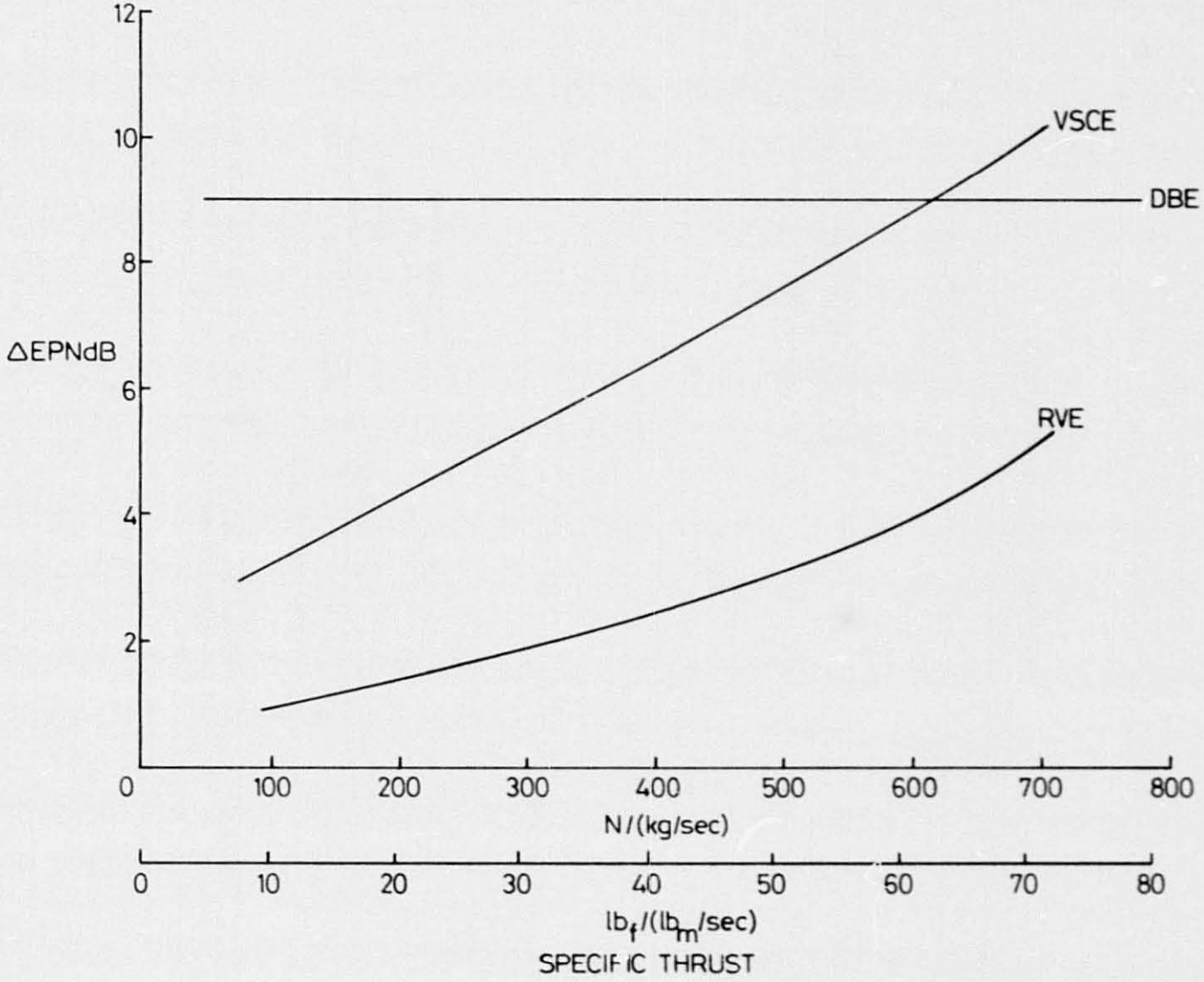

Figure B5.- Incremental noise suppression due to annular/coannular noise relief.

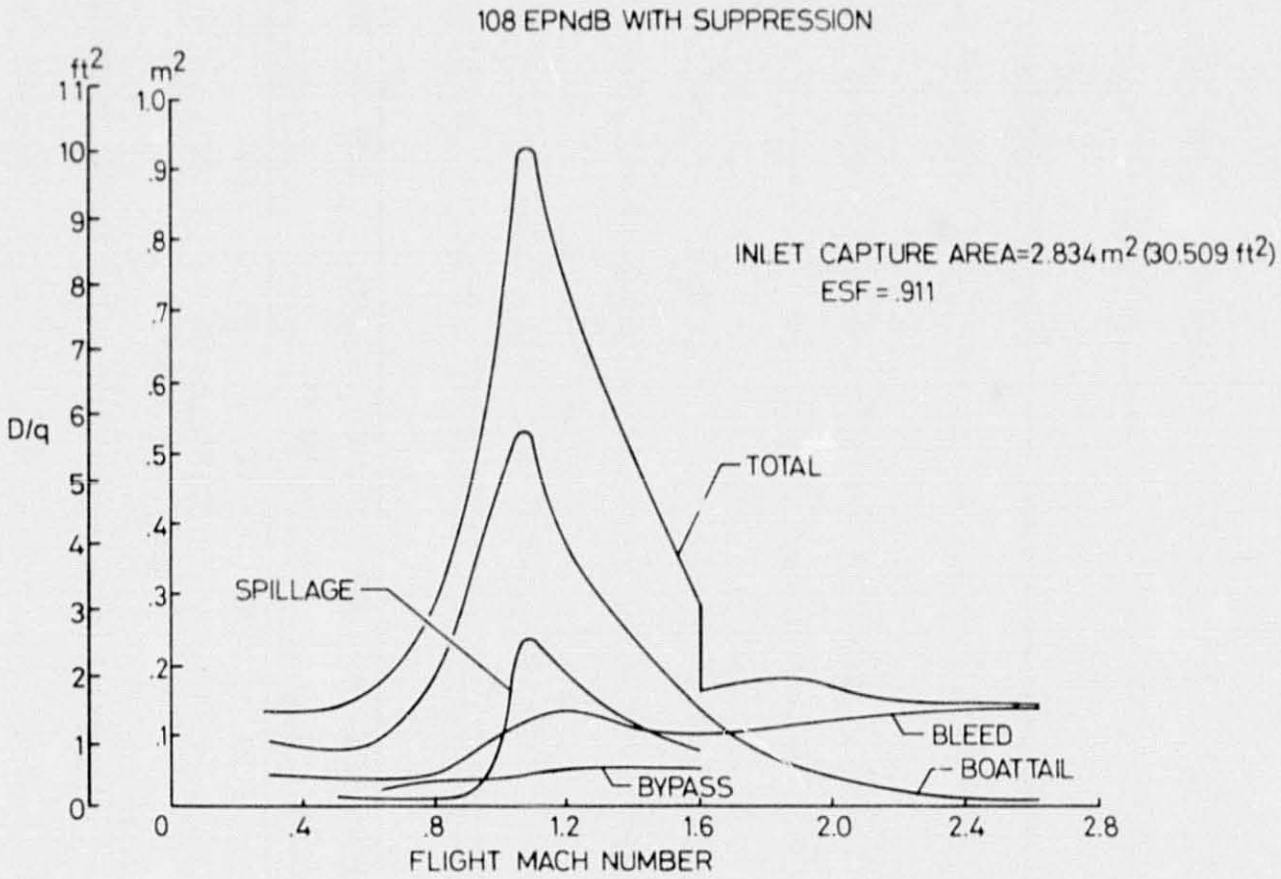

Figure C1.- VSCE propulsion system drag to dynamic pressure ratio for maximum non-augmented power - Climb trajectory.

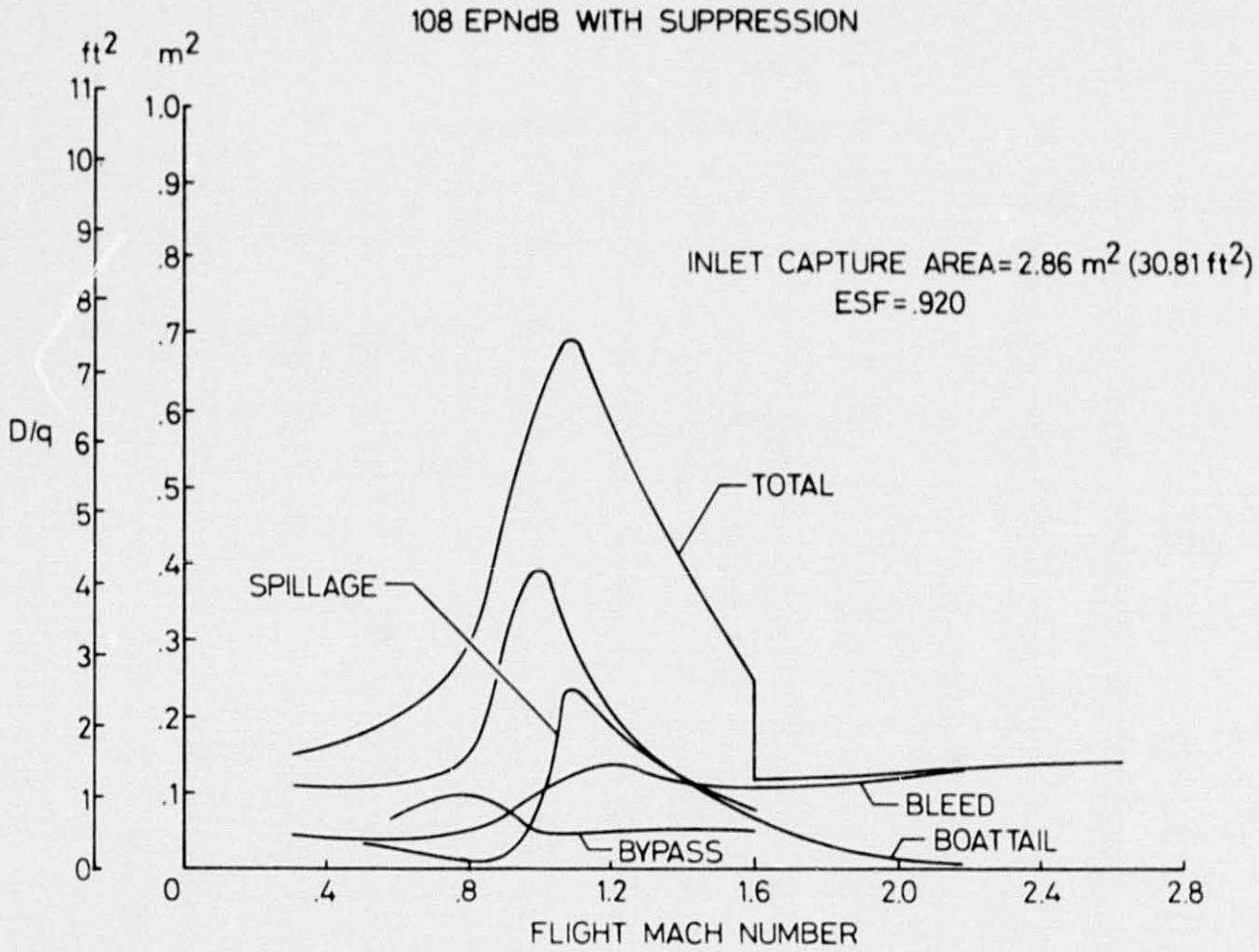

Figure C2.- RVE propulsion system drag to dynamic pressure ratio for turbojet mode - Climb trajectory.

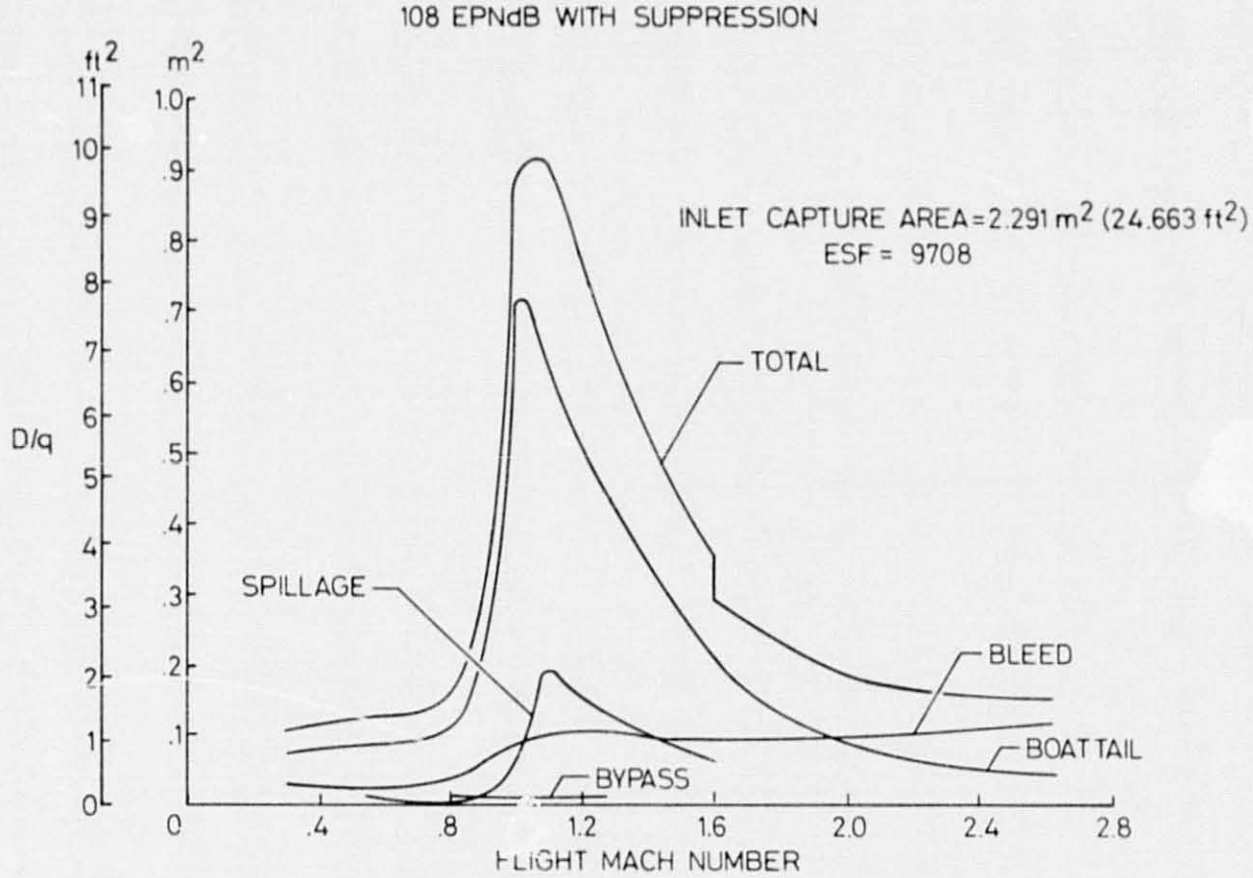

Figure C3.- DBE propulsion system drag to dynamic pressure ratio for maximum non-augmented power - Climb trajectory.

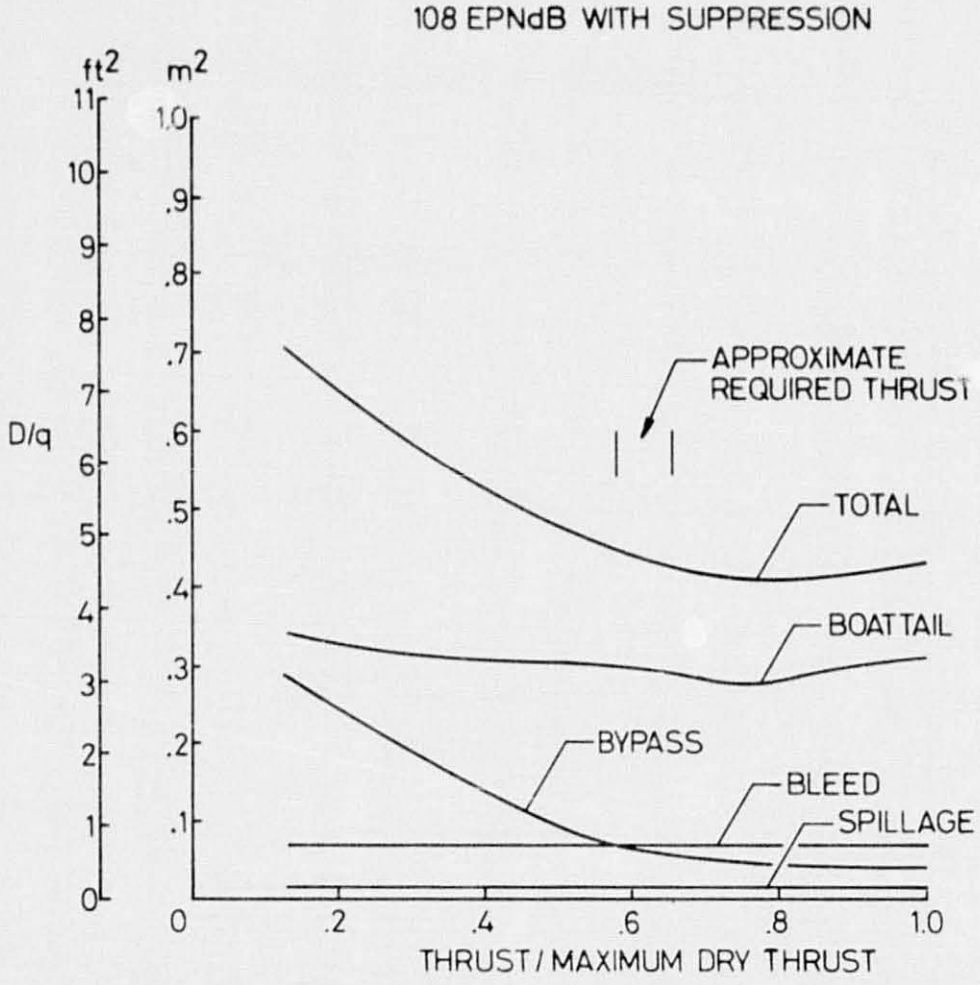

Figure C4.- VSCE propulsion system drag to dynamic pressure ratio - M = 0.9 stratosphere.

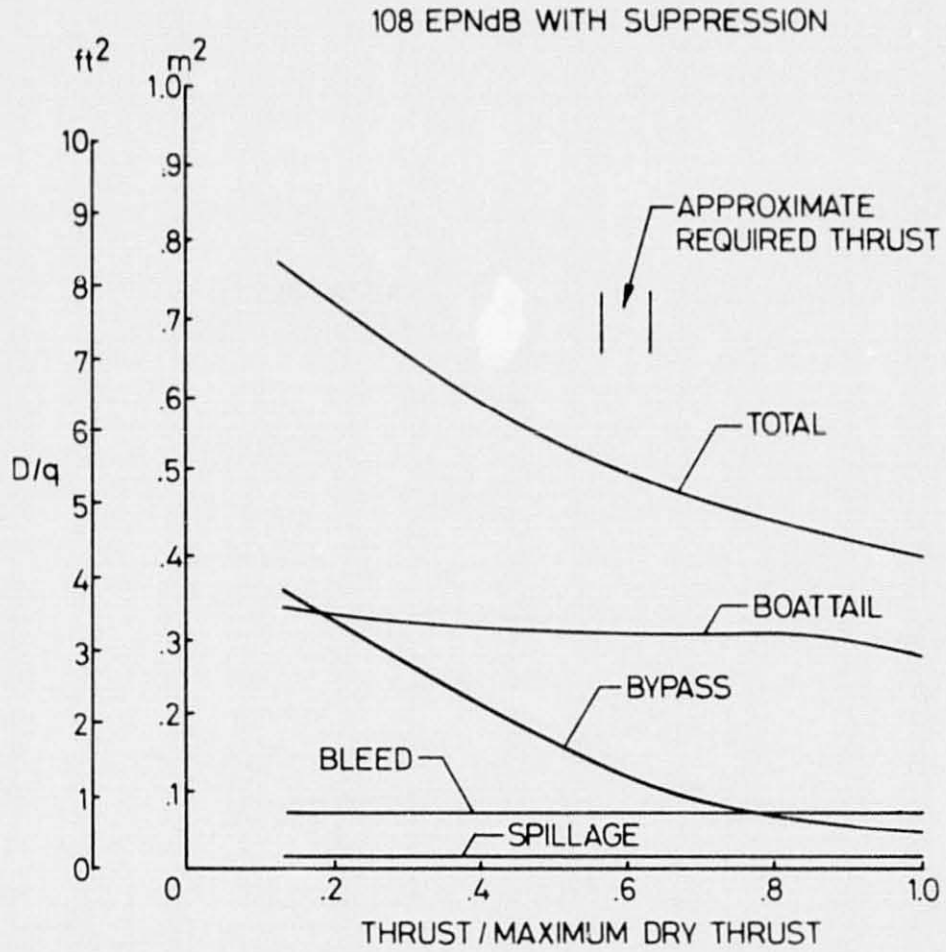

Figure C5.- RVE propulsion system drag to dynamic pressure ratio - M = 0.9 stratosphere.

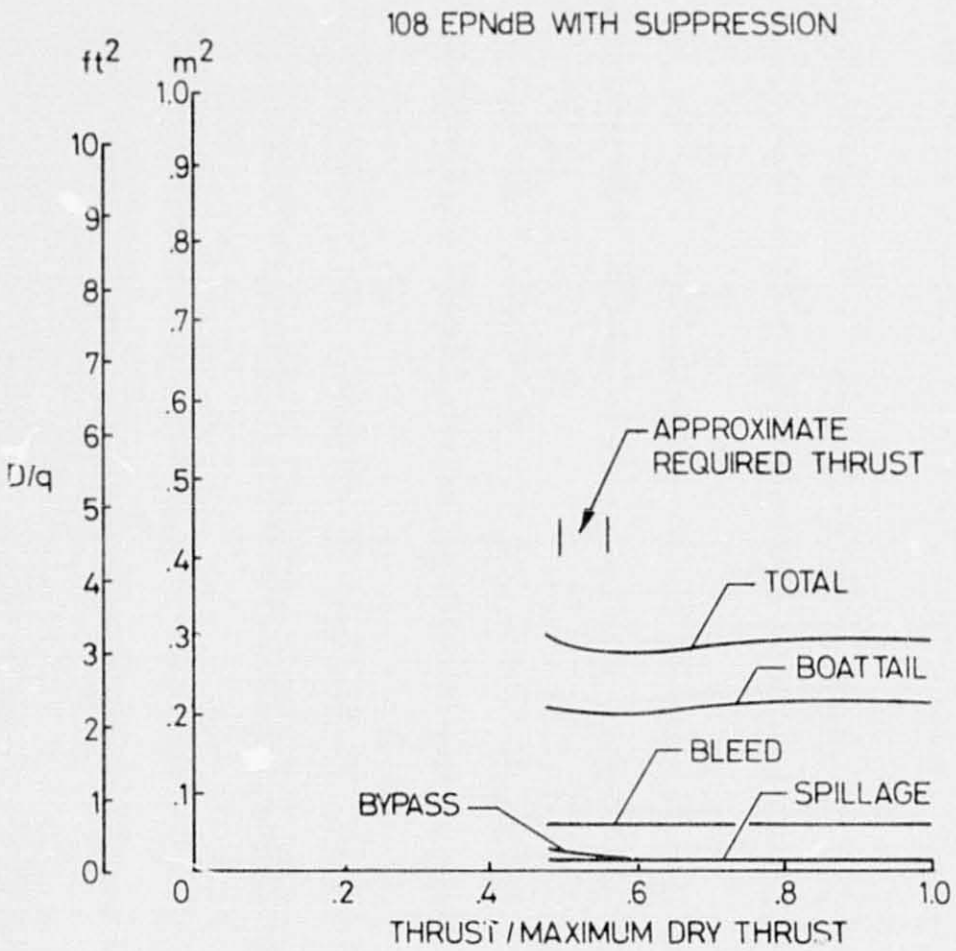

Figure C6.- DBE propulsion system drag to dynamic pressure ratio - M = 0.9 stratosphere.